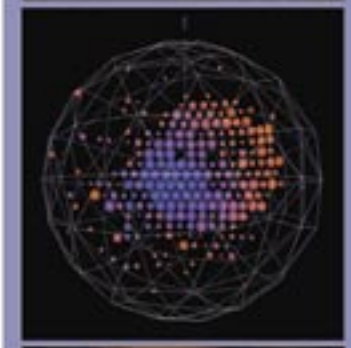

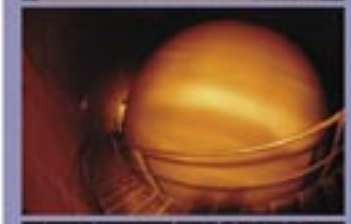

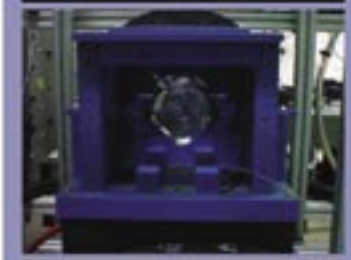

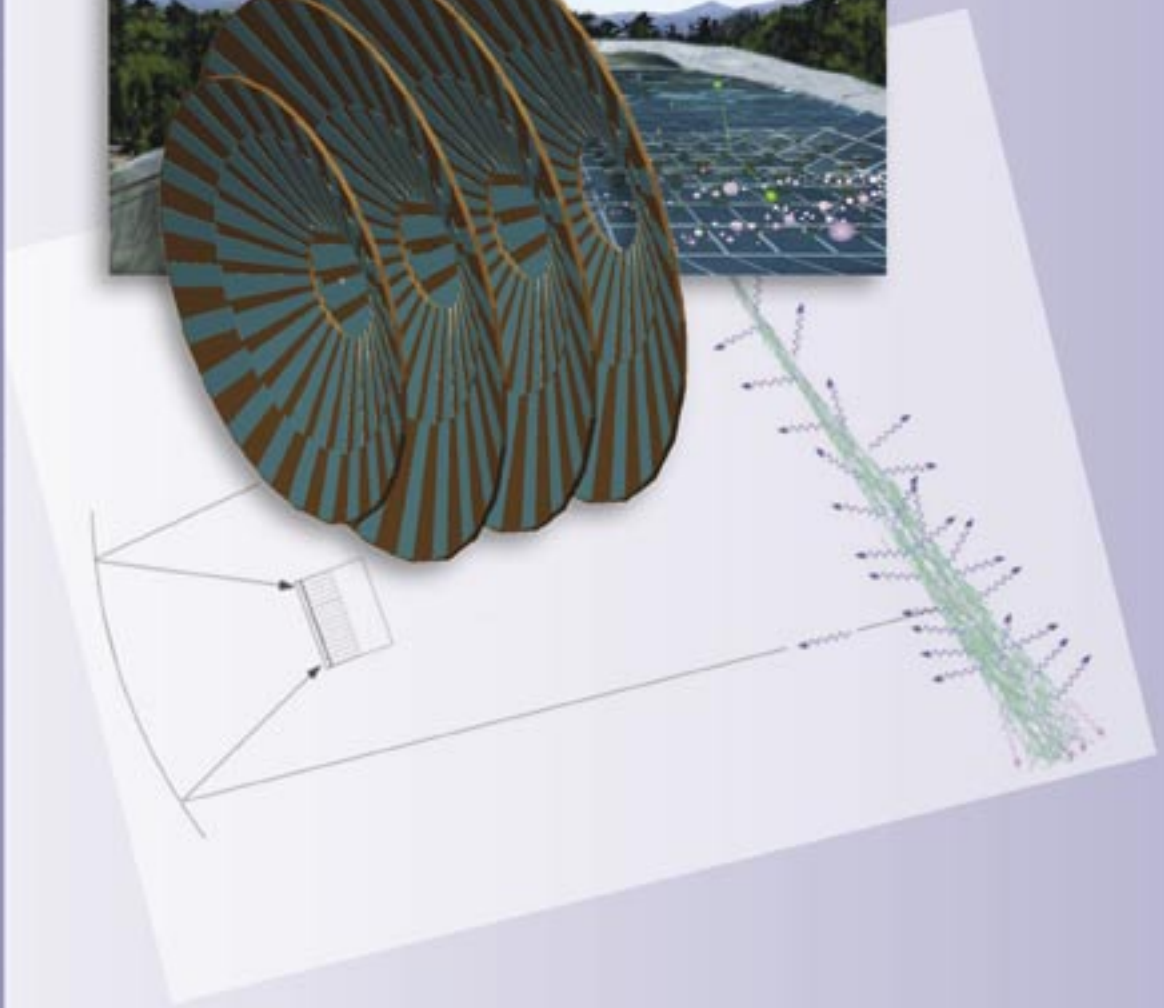

Nuclear Physics and Astrophysics

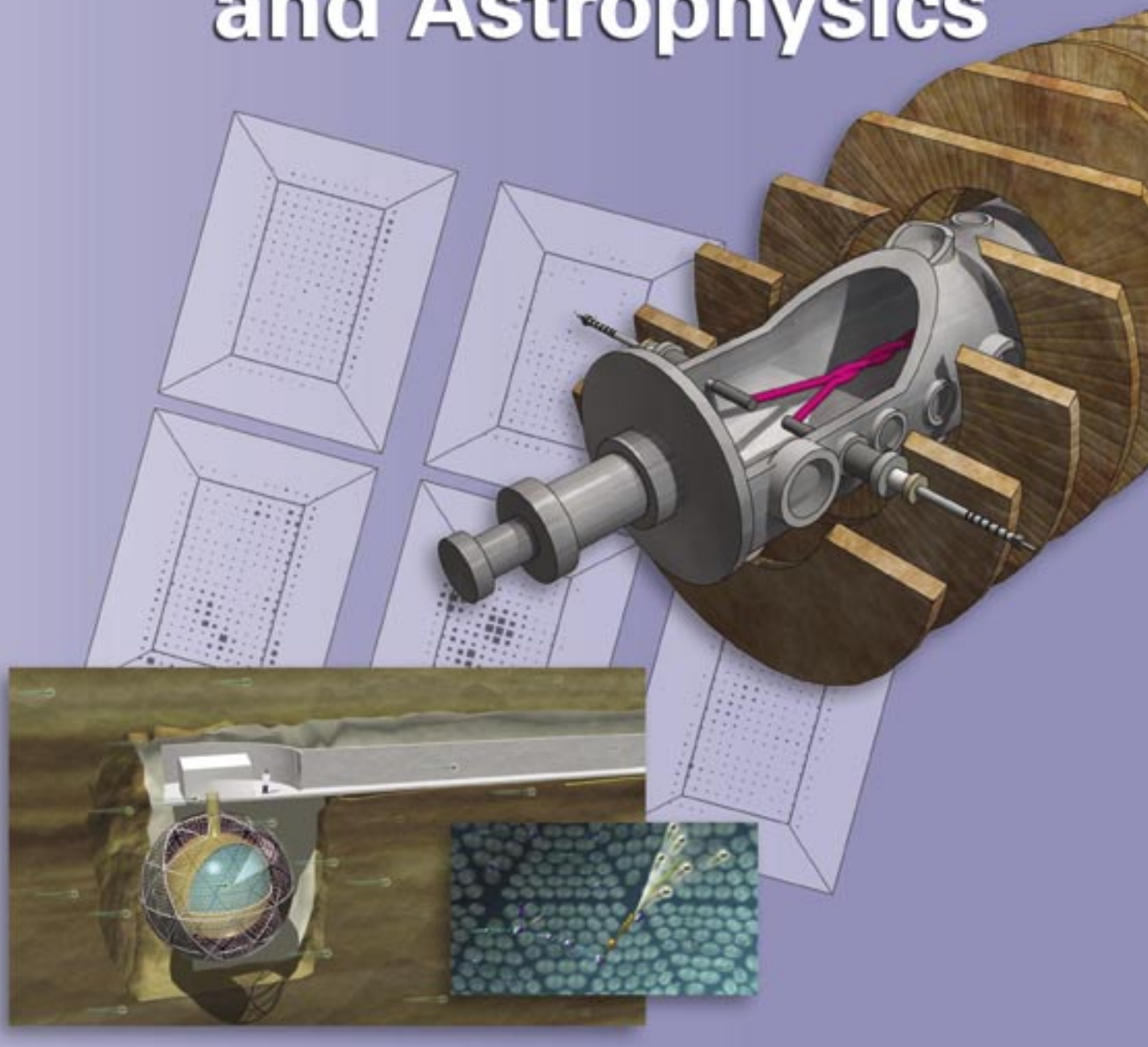

Nuclear Physics and Astrophysics Contents

Research Highlights

Project Descriptions

The Sudbury Neutrino Observatory—Taking Physics Beyond the Standard Model

A. Hime, M.G. Boulay, T.J. Bowles, M.R. Dragowsky, S.R. Elliott, A.S. Hamer, J.C. Heise (P-23), M.M. Fowler, G.G. Miller, J.B. Wilhelmy (C-INC), J.M. Wouters (IM-8), R. Van de Water (P-25)

In the 1930s, in an attempt to preserve the conservation of energy in nuclear beta decay, Wolfgang Pauli invented a new particle—the neutrino. This elusive particle has no electric charge and interacts so weakly that it was almost impossible to detect. More than 20 years later, the neutrino was finally observed by a research team from LANL in an experiment at the Hanford reactor. Two years later, a definitive experiment at the Savannah River reactor clearly demonstrated the existence of the neutrino. Subsequent measurements at various facilities indicated that neutrinos come in at least three different types, or "flavors"—electron, muon, and tau. Determining whether neutrinos have mass is an issue of great importance to particle physics, astrophysics, and cosmology. The search for evidence of neutrino mass and the study of neutrino interactions with nuclei has evoked continuous experimental efforts by scientists from LANL for over 50 years. Accelerator-driven neutrino experiments like those performed on the LSND at LANSCE and now the BooNE (which is currently taking data at FNAL in Illinois to definitively test the LSND findings) provide evidence that could indicate that neutrinos do, in fact, oscillate from one type to another and therefore have mass (see *Accelerator Neutrino Experiments on the LSND and MiniBooNE*, p. 131, in this report). We are performing non-accelerator-based experiments using SNO—a terrestrial detector located 6,800 ft underground in an active nickel mine in Ontario, Canada—to understand why solar neutrino fluxes measured in terrestrial detectors fall significantly short of standard solar model predictions.[1] Both accelerator- and non-accelerator-driven neutrino experiments provide important tests that may challenge the Standard Model of electro-weak interactions while searching for neutrino oscillations.

Resolving the Solar-Neutrino Puzzle

While continuing to probe the neutrino at accelerators, LANL scientists initiated a program of non-accelerator physics that provided alternative means to probe the properties of the neutrino. A high-precision measurement of the spectrum of the electrons emitted in the beta decay of tritium provided a means to search for a very small neutrino mass. This experiment provided a limit on the mass of the electron-type neutrino, which was sufficient to rule out electron-type neutrinos as being the dominant mass in the universe. To dramatically improve sensitivity, scientists shifted the focus of non-accelerator efforts to measurements of solar neutrinos produced 93 million miles away—deep in the nuclear furnace of the sun. LANL played the lead role in a solar-neutrino experiment, known as the Soviet-American Gallium Experiment (SAGE), at the Baksan Neutrino Observatory in the Caucusus mountains of southern Russia.[2] SAGE uses

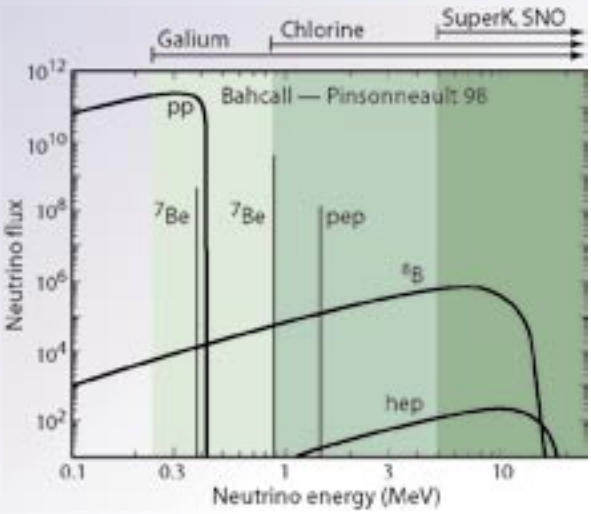

Figure 1. The solar-neutrino energy spectrum as computed by Bahcall and Pinsonneault.[3] Terrestrial-solar-neutrino experiments have measured neutrinos from the sun across the entire energy spectrum. The low-energy radiochemical experiments determine an integral flux of solar neutrinos above their respective thresholds. The water Cerenkov detectors, SuperKamiokande (SuperK) and SNO, measure the ^{8}B flux of solar neutrinos directly.

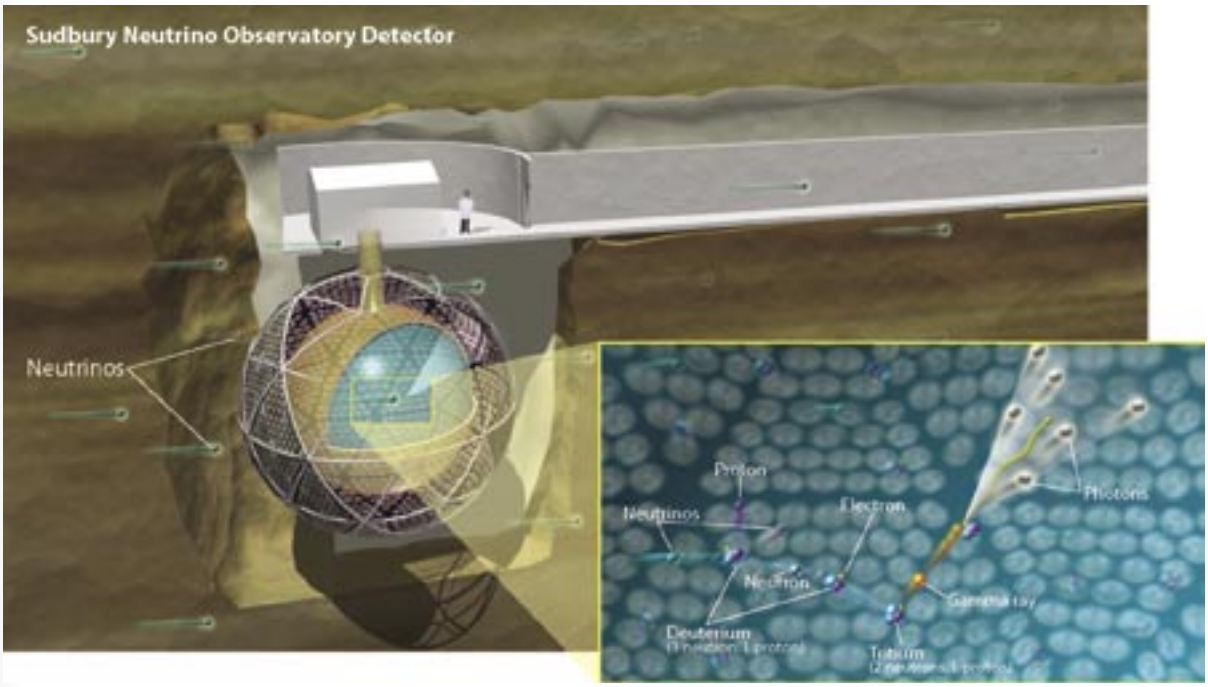

Figure 2. Three-dimensional rendering of SNO. In one of three neutrino reactions (in the inset) detected by SNO, a neutrino entering the detector interacts with a deuterium nucleus. The reaction produces a proton, neutrino, and neutron. The neutron is captured by another deuterium nucleus, producing a tritium atom in the process. The tritium atom decays and in that process releases a gamma ray, which then collides with an electron. Cerenkov light is emitted and detected by PMTs that line inside of the SNO vessel.

50 tons of metallic gallium in which the neutrinos that drive the primary energy-producing fusion reaction in the sun whereby two protons (p-p) fuse to form deuterium can transform the ^{71}Ga nuclei into ^{71}Ge. The individual atoms of germanium that are formed are chemically extracted and counted when they decay back to ^{71}Ga. This measurement provided the first determination of the total flux of neutrinos from the sun and produced a very significant finding—the reduction in flux that had been observed in high-energy neutrinos also extends down to low-energy neutrinos. Measurements of the visible solar luminosity determine uniquely how many of the low-energy p-p neutrinos are produced in the sun. The SAGE results are very hard to understand unless neutrinos oscillate and provide a critical ingredient in resolving the puzzle of the missing solar neutrinos.

For more than three decades, solar-neutrino experiments have been performed in parallel with detailed SSM predictions of the solar-neutrino flux and energy spectrum.[3] With data spanning essentially the entire solar-neutrino spectrum (Figure 1), a Solar Neutrino Puzzle (SNP) emerges wherein the fluxes measured in terrestrial detectors fall significantly short of SSM predictions.[1] The SSM is constrained by knowledge of the solar luminosity and is now independently tested using helioseismology. The data are inconsistent with a sun that "shines" based upon our basic notions of stellar evolution and the basic tenets of nuclear and particle physics—which hint of new physics not contained in the present Standard Model of elementary particles. In particular, electron neutrinos born in nuclear fusion reactions powering the sun are thought to somehow transform into different types of neutrinos that go undetected in experiments on the earth—a hypothesis known as *neutrino-flavor transformation.*[4] Because the sun is energetic enough to produce only electron neutrinos and because, until recently, terrestrial detectors are sensitive largely only to electron neutrinos, the SNP can be resolved if sun-born electron neutrinos are somehow transformed to muon and/or tau neutrinos before their arrival on the earth. Testing neutrino-flavor transformation requires a solar-neutrino detector that can detect the disappearance of electron neutrinos and the appearance of muon and/or tau neutrinos.

The SNO experiment may realize the possibility of neutrino-flavor transformations. At the heart of the SNO detector is 1,000 tonnes of ultra-pure heavy water (D_2O), which serves as a neutrino target. Neutrino interactions are identified through the production of Cerenkov light detected in an array of 10,000 PMTs (Figure 2). The SNO experiment exploits three unique interactions of ^{8}B solar neutrinos on deuterium (^{8}B is an element produced in the sun; it beta decays to produce electron neutrinos):

(CC) $\nu_e + d \rightarrow p + p + e^- - 1.44$ MeV,

(ES) $\nu_x + e^- \rightarrow \nu_x + e^-$, and

(NC) $\nu_x + d \rightarrow p + n + \nu_x - 2.22$ MeV.

The charged-current (CC) interaction can proceed only with electron neutrinos incident on deuterium, whereas the neutral-current (NC) interaction can proceed with equal probability for all active neutrino flavors. The elastic-scattering (ES) interactions are also sensitive to all active neutrino flavors; however, the cross-section is about 6.5 times larger for electron neutrinos than for muon and/or tau neutrinos. The basic concept relies on a direct comparison of the CC flux to that measured in the ES and/or NC channels. A measurement of high ES and/or NC fluxes relative to the CC flux would provide a smoking gun for active neutrino-flavor transformation of electron neutrinos into muon and/or tau neutrinos.

SNO is a heavy-water Cerenkov detector that took over a decade in the making with some 100 collaborators in Canada, the U.S., and the United Kingdom (Figure 2). Its results are best represented in terms of the *flavor content* of the ^{8}B solar-neutrino flux depicted in Figure 3. In the simplest sense, the 35-year-old SNP is resolved with data from the SNO experiment. The deficit of electron neutrinos born in the sun is a result of flavor transformation into muon and/or tau neutrinos that are now detected at earth through the unique NC interaction in SNO. Moreover, the total flux of ^{8}B neutrinos extracted from this measurement is in very good agreement with predictions of the SSM. Consequently, our basic concepts of how the sun shines appear intact, and we have witnessed the discovery of new physics in the guise of solar-neutrino flavor transformation. We now know that this flavor transformation definitely results because neutrinos have non-zero mass and that neutrino oscillations occur in nature.

Conclusion

Present and future plans for SNO. These milestone results from SNO were obtained while operating the detector during the "pure-D_2O" phase from November 2, 1999, through May 28, 2001.[5,6,7] The NC rate of solar neutrinos was deduced by counting the neutrons liberated when neutrinos disintegrate the deuteron. In D_2O, this signal ensues from the Cerenkov light produced when these neutrons recapture on deuterium and create 6.25-MeV gamma rays in the process. Significant improvements in precision can be made in the "dissolved-salt" phase in SNO whereby the detector is operated after dissolving 2 tonnes of NaCl into the 1,000-tonne D_2O volume. In addition, because of the multi-gamma cascade associated with neutron capture on chlorine, an additional degree of freedom, or "event isotropy," allows for better separation of the various solar-neutrino signals. The SNO detector has been operating in the dissolved-salt phase since mid May 2001. Results from the dissolved-salt phase have recently been released[8]; these results improve sensitivity to the NC by about a factor of three over the pure-D_2O phase with significant improvement in the constraints on fundamental neutrino parameters (Figure 4).

Ultimately, the CC and NC signals will be independently and simultaneously extracted in SNO by detecting neutrons in a discrete array of neutral current detectors (NCDs) comprised of some 400 m of ultra-low-background ^{3}He proportional counters. A research and development program was started over a decade ago at LANL to develop an NCD array with intrinsically low radioactivity and with the capability of operating effectively under water. In collaboration with colleagues at the University of Washington and Lawrence Berkeley Laboratory, we have completed a full-scale construction of the NCD array. Plans are under way to deploy the array into SNO now that the dissolved-salt phase is complete.

New-generation experiments. With data from the SNO experiment, the 35-year-old SNP is resolved, and we now know that neutrinos have mass and that neutrino oscillations occur. Improvements in precision measurements at SNO will better define the neutrino mass and mixing parameters and further test our models of stellar evolution. Nonetheless, fundamental questions remain for the neutrino sector that cannot be addressed in existing experiments.

The evidence for neutrino oscillations described above constrains the flavor-mixing parameters but only for the splitting of the mass between the different neutrino states. Determining the absolute mass scale for the neutrinos (which is now known to be very small relative to the other elementary particles in nature) is also interesting. One exciting possibility for determining the absolute scale of neutrino mass is zero-neutrino double-beta decay. Two-neutrino double-beta decay is a second-order weak process that has been observed

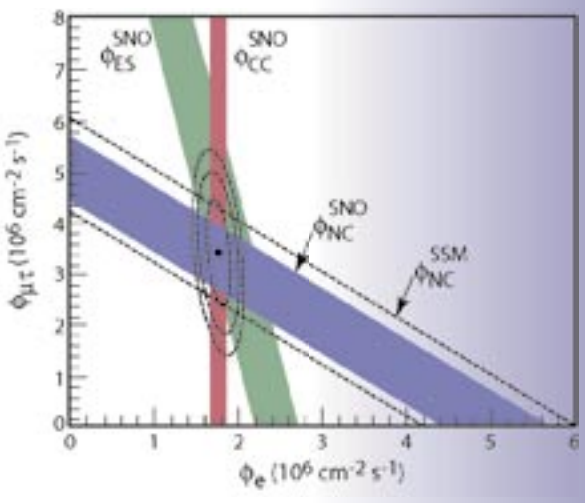

Figure 3. Flavor-content analysis of the ^{8}B solar-neutrino flux based upon data from the SNO experiment. Two-thirds of the electron neutrinos born in the sun disappear because of active neutrino-flavor transformation whereby they reappear as muon and/or tau neutrinos in the SNO detector. The total flux of ^{8}B neutrinos is in very good agreement with SSM calculations.

although it is very rare. A typical half-life is 10^{20} years, which is long compared to the age of the universe (~ 10^{10} years). A more interesting process, if it exists, is neutrinoless double-beta decay. This process, where no neutrinos are emitted, requires special characteristics of the neutrino and incorporates a two-step process. In both steps of this exchange, an electron would be emitted; however, no neutrino is released. For the exchange to take place, there must be no distinction between a neutrino and an anti-neutrino. If the neutrino has this property, we refer to it as a *Majorana* neutrino. Additionally, neutrinoless double-beta decay requires that neutrinos be the massive Majorana flavor. The Majorana Project at LANL will use 500 kg of enriched ^{76}Ge to search for this rare process with unprecedented precision.

In addition to the Majorana project, new research and development efforts are also under way at LANL to obtain a detector that can detect low-energy solar neutrinos in real time. About 90% of the solar-neutrino flux is contained below an energy threshold of 1 MeV, which is far below the achievable threshold of a Cerenkov detector such as SNO. A detector with such low-energy capability would serve as the best means for a precision measurement of neutrino parameters and would test models of stellar evolution at the 1% level. Interestingly enough, such detectors, including perhaps the Majorana detector, could serve a valuable dual role. If the intrinsic radioactivity of these detectors can be achieved with a very-low-energy threshold, then they can also be used to intensively search for the missing energy (or dark matter) of the universe.

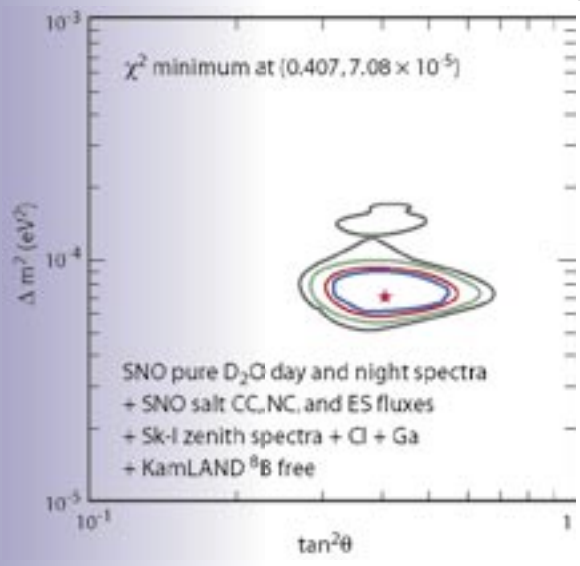

Figure 4. Constraints on the solar-neutrino mass and mixing parameters based on a global fit to all existing solar-neutrino and reactor-neutrino data. The central star indicates the best-fit value as indicated by the parameters found at minimum chi-square. Contours are shown at the 90%, 95%, 99%, and 99.73% confidence levels.

References

1. A. Hime, "Exorcising ghosts–In pursuit of the missing solar neutrinos," *Celebrating the Neutrino, Los Alamos Science* **25**, 137-151 (1997).
2. T.J. Bowles, "The Russian-American gallium experiment," *Celebrating the Neutrino, Los Alamos Science* **25**, 152-155 (1997).
3. J.N. Bahcall, *Neutrino Astrophysics* (Cambridge University Press, 1989).
4. R. Slansky, S. Raby, T. Goldman, and G. Garvey, "The oscillating neutrino–An introduction to neutrino masses and mixing," *Celebrating the Neutrino, Los Alamos Science* **25**, 28-77 (1997).
5. SNO Collaboration, "Measurement of the rate of electron neutrino interactions produced by ^{8}B solar neutrinos at the Sudbury Neutrino Observatory," *Physical Review Letters* **87**, 071301 (2001).
6. SNO Collaboration, "Direct evidence for neutrino flavor transformation from neutral-current interactions in the Sudbury Neutrino Observatory," *Physical Review Letters* **89**, 011301 (2002).
7. SNO Collaboration, "Measurement of day and night neutrino energy spectra at SNO and constraints on neutrino mixing parameters," *Physical Review Letters* **89**, 011302 (2002).
8. SNO Collaboration, "Measurement of the total ^{8}B solar neutrino flux at SNO with enhanced neutral-current sensitivity," to appear in *Physical Review Letters* (2003).

Acknowledgment

We gratefully acknowledge the support of the DOE Office of Nuclear Physics and the LANL LDRD Program.

For more information, contact Andrew Hime at 505- 667-0191, ahime@lanl.gov.

Accelerator Neutrino Experiments on the LSND and MiniBooNE

W.C. Louis III (P-25), representing the LSND and MiniBooNE Collaborations

The neutrino is one of the most elusive particles in the universe, yet it exists in great abundance and is a fundamental element in the universe's subatomic structure. Because these low-energy particles interact weakly with other particles, neutrinos had defied detection for years until 1953 when LANL scientists Fredrick Reines (Figure 1) and Clyde Cowan, Jr., detected these elusive particles in experiments that used liquid scintillator detectors at reactors in Washington and South Carolina. The neutrino, originally thought to be massless, exists in three distinct states (commonly called "flavors")—electron, muon, and tau forms.

LANL researchers used the LSND[1] from 1993–1998 to conduct experiments designed to collect data and obtain evidence that neutrinos oscillate from the muon neutrino form into the electron neutrino form. Neutrino oscillations are the transformation of one neutrino flavor into another neutrino flavor, and these transformations occur only if neutrinos have mass and if there is mixing among the neutrino flavors. The LSND results imply that neutrinos constitute at least 1% of the universe's total mass. MiniBooNE,[2] which is now operational at FNAL in Illinois, is the first phase of the larger BooNE that will definitively test the LSND evidence for neutrino oscillations and precisely measure the oscillation parameters. MiniBooNE is looking for oscillations of muon neutrinos (ν_μ) into electron neutrinos (ν_e). A large tank filled with mineral oil (CH_2) is used to look for particles produced when neutrinos hit the nuclei of the atoms that make up the oil. The signature of such an interaction is a cone of light, known as Cerenkov light, which hits light-sensitive devices (PMTs) mounted on the inside surface of the tank. If successful, MiniBooNE will provide a unique environment to observe physics beyond the Standard Model.

Figure 1. Fred Reines working on an underground neutrino experiment at a South African mine in 1966 (photo courtesy of the University of California, Irvine).

LSND—The Foundation for Future Neutrino Research

The LSND experiment was designed to search for oscillations of muon antineutrinos to electron antineutrinos ($\bar{\nu}_\mu \rightarrow \bar{\nu}_e$) from positively charged muon (μ^+) decay at rest (DAR) with high sensitivity. (The LSND collaboration consisted of groups from eleven organizations, including LANL). Over the six-year running period from 1993–1998, the LANSCE accelerator delivered 28,896 C (~ 0.3 g) of protons to the production target. The resulting DAR neutrino fluxes were well understood because almost all detectable neutrinos arose from positively charged pion (π^+) or μ^+ decay.

The LSND was an 8.3-m-long, 5.7-m-diam cylindrical tank that contained 167 tons of mineral

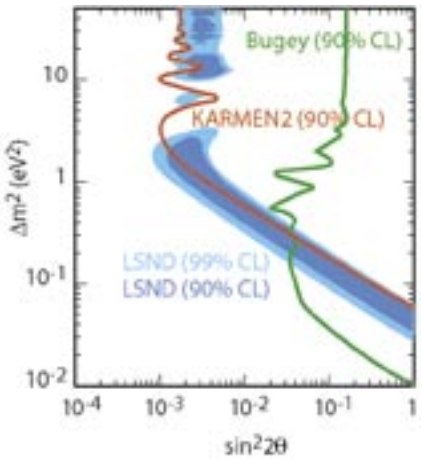

Figure 2. The ($sin^2 2\theta, \Delta m^2$) oscillation parameter fit for the entire LSND data sample. (CL is "confidence level.")

oil with a dab of scintillating compound to amplify light signals used to reconstruct neutrino events. The Cerenkov light (described later) from these events was detected by 1,220 PMTs (each 8 in.) located on the inside surface of the LSND tank. The PMTs convert the light into electrical signals, which are gathered and interpreted by data-acquisition computers. The center of the LSND was 30 m from the neutrino source. The main veto shield consisted of a 15-cm layer of liquid scintillator in an external tank and 15-cm layer of lead in an internal tank. Designed to search for the presence of electron antineutrinos with great sensitivity, the LSND witnessed over 80 neutrino events that were consistent with muon antineutrinos oscillating into electron antineutrinos.

The primary neutrino-oscillation search in LSND was for $\overline{\nu}_\mu \rightarrow \overline{\nu}_e$ (i.e., a muon antineutrino to an electron antineutrino), where the $\overline{\nu}_\mu$ arise from DAR μ^+ in the beam stop, and the ν_e are identified through the reaction $\overline{\nu}_e p \rightarrow e^+ n$. This reaction allowed a two-fold signature of a positron with a 52.8-MeV endpoint and a correlated 2.2-MeV gamma ray (γ) from neutron capture on a free proton. More events were observed than expected, and the excess was consistent with neutrino oscillations.

Figure 2 shows the ($sin^2 2\theta, \Delta m^2$) oscillation parameter fit for the entire data sample, $20 < E_e < 200$ MeV. The mixing angle between the two neutrinos is "$sin^2 2\theta$," and the difference in masses squared of the two neutrinos is "Δm^2." The fit includes both $\overline{\nu}_\mu \rightarrow \overline{\nu}_e$ and $\nu_\mu \rightarrow \nu_e$ oscillations and all known neutrino backgrounds. The inner and outer regions correspond to 90% and 99% confidence-level allowed regions, whereas the curves are 90% confidence-level limits from the Bugey reactor experiment and the KARMEN2 experiment at ISIS, the Rutherford-Appleton Laboratory Neutron Facility in the United Kingdom. The allowed region that is most favorable is the band from 0.2–2.0 eV^2, although a region around 7 eV^2 is also possible.

MiniBooNE—The First Phase for Confirmation of Neutrino Oscillations

The MiniBooNE detector consists of a 12-m-diam spherical tank contained within a cylindrical vault (Figure 3a and b). An inner tank supports 1,280 individual PMTs pointed inward and optically isolated from the tank's outer region, which contains an additional 240 PMTs (Figure 3c). The inner tank is filled with 800 tons of mineral oil, which is the equivalent of 44 tanker trucks filled with liquid. An outer tank serves as a veto shield for identifying particles both entering and exiting the detector. MiniBooNE is located ~ 500 m from FNAL's neutrino source, and it detects one neutrino collision every 20 s. For this first phase of the experiment, we expect to detect one million neutrino events per year.

In MiniBooNE, the 8-GeV protons from FNAL's Booster accelerator interact with the atoms in a beryllium target located inside a magnetic focusing horn (Figure 4). (The Booster accelerator can reliably deliver protons for most of a calendar year, which allows the experiment to receive up to ~ 5×10^{20} protons per year.) The positively charged

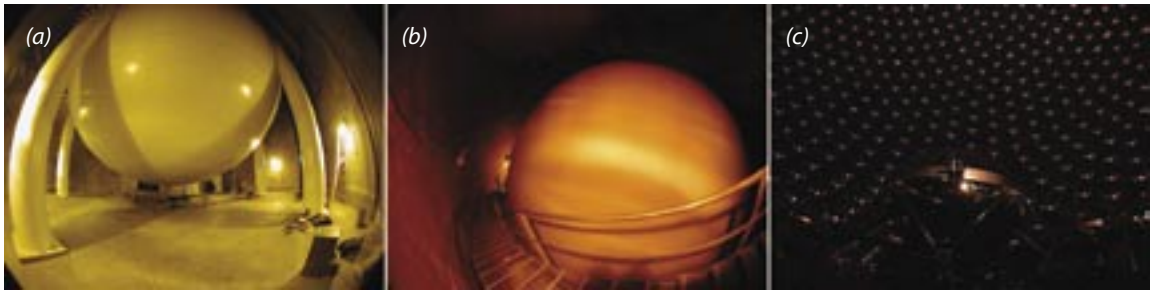

Figure 3. The MiniBooNE detector tank viewed from the floor (a) and from the stairway (b) in the underground vault. (c) A portion of the PMTs installed inside the detector.

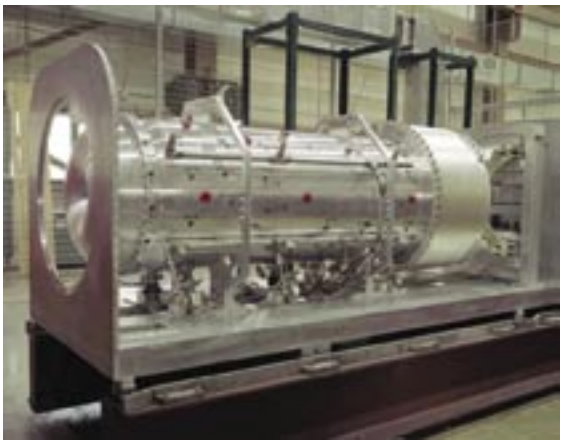

Figure 4. FNAL's magnetic focusing horn. The beryllium target that produces pions through proton interactions with the target material is located in the upstream position inside the horn.

pions (π) produced from these interactions are focused by the magnet horn into a 2-m-diam, 50-m-long steel pipe where they decay into muon neutrinos (ν_μ). At the end of the decay pipe, a concrete/steel absorber stops all particles except the muon neutrinos, which continue through ~ 450 m of earth to reach the detector tank. The muon neutrinos—delivered in bursts that last 1.6 millionths of second, 5 times per second—collide with carbon atoms in the mineral oil, producing muons (μ^+). These subatomic charged particles create cones of Cerenkov light—a key factor in these experiments—as they travel through the mineral oil. (Cerenkov light is essentially the electromagnetic equivalent of a sonic boom. It travels to the edges of the detector tank where the PMTs receive the light and convert it to electrical signals.)

Some of the muon neutrinos entering the detector tank can oscillate into electron neutrinos (ν_e) *before* they collide with carbon atoms. If this occurs, electrons (instead of energetic muons) will be produced when the electron neutrinos collide with the carbon atoms in the mineral oil. The electrons scatter and quickly come to rest after colliding with atoms in the mineral oil. The subsequent Cerenkov cone of light is distinct (i.e., the inner and outer edges of the cone are hazy) from that produced by other interactions within the detector tank. If MiniBooNE verifies the LSND experiment, then approximately 1,000 $\nu_e C \rightarrow e^- X$ events should be observed above background from $\nu_\mu \rightarrow \mu_e$ oscillations. There are three main backgrounds to the oscillation search: (1) intrinsic ν_e background in the beam from μ and K (kaon) decay in the decay pipe, (2) misidentified μ events ($\nu_\mu C \rightarrow \mu^- X$), and (3) misidentified π^0 (pion) events ($\nu_\mu C \rightarrow \nu_\mu \pi^0 X$). Figure 5 shows the expected oscillation sensitivity for the two-year ν_μ or $\overline{\nu}_\mu$ run cycle.

The MiniBooNE detector and beam are now fully operational and taking data. The detector was calibrated with laser-calibration events; the energy scale and resolution were determined from cosmic-muon and Michel-electron events, and approximately 160,000 clean neutrino events were recorded after the first year of data taking with about 1.5×10^{20} protons on target. At present, the experiment is clearly reconstructing both $\nu_\mu C \rightarrow \mu^- X$ charged-current events and $\nu_\mu C \rightarrow \nu_\mu \pi^0 X$ neutral-current events, which are the two main backgrounds to the $\nu_\mu \rightarrow \nu_e$ oscillation search. As shown in Figure 5, π^0 events are being reconstructed at approximately the correct mass with a mass resolution of about 21 MeV.

The current plan is to run the first two full years (1×10^{21} protons on target) with ν_μ and then switch to a $\overline{\nu}_\mu$ run cycle. First results are expected by 2005, and if the LSND oscillation signal is confirmed, a BooNE detector will then be built at a different distance than the MiniBooNE detector to obtain the highest precision measurement of the oscillation parameters.

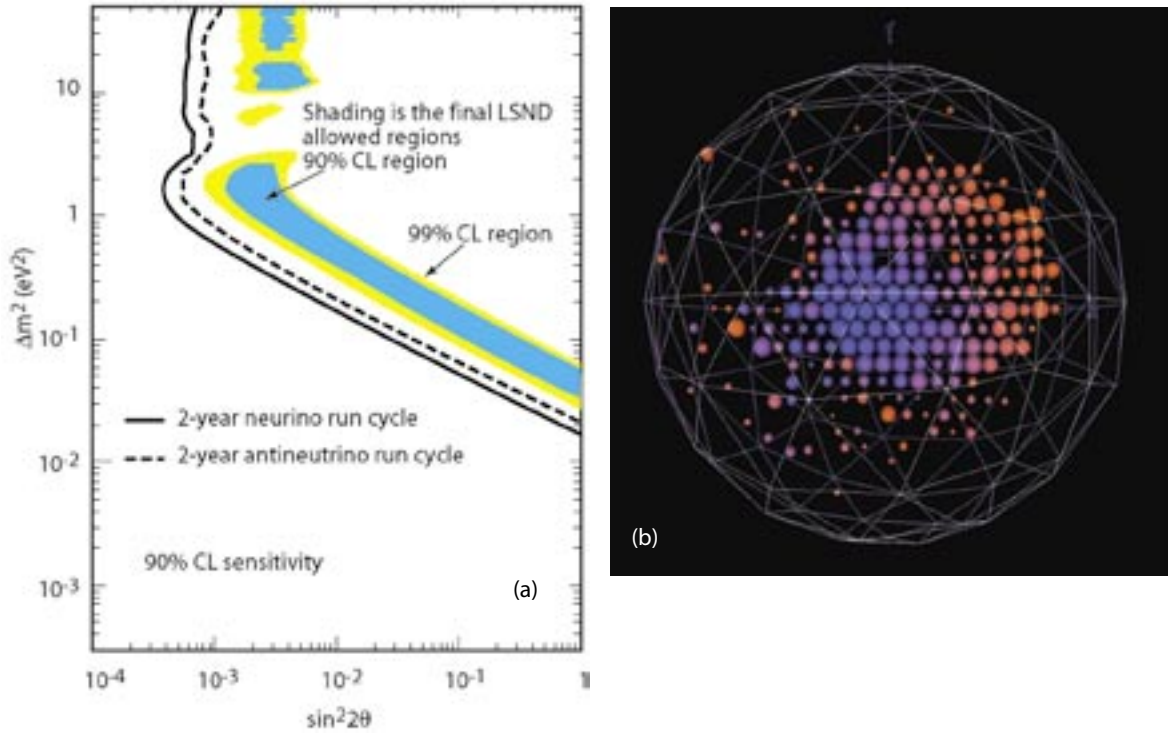

Figure 5. (a) The MiniBooNE expected oscillation sensitivity for a full two-year run cycle. (CL is "confidence level.") (b) A typical MiniBooNE neutrino-induced event. The colors relate to elapsed time; the blue represents early PMT hits and the orange reprsents later PMT hits. In this particular data event, there were less than 6 veto hits and over 200 tank hits.

Conclusion

The confirmation of neutrino oscillations at high Δm^2 would have a huge impact on astrophysics, as well as particle and nuclear physics. When combined with the evidence for neutrino oscillations from solar and atmospheric neutrino experiments, the present data seem to imply physics beyond the Standard Model, such as the existence of light, sterile neutrinos or the violation of CPT. (CPT is the combined operation of charge conjugation, parity inversion, and time reversal.) The MiniBooNE experiment at Fermilab will provide a definitive test of the LSND evidence for neutrino oscillations.

References

1. A. Aguilar *et al.*, *Physical Review D* **64**, 112007 (2001).
2. E. Church *et al.*, "A proposal for an experiment to measure $\nu_\mu \rightarrow \nu_e$ oscillations and ν_μ disappearance at the Fermilab booster: BooNE," LANL report LA-UR-98-352 (FNAL experiment 898); A. O. Bazarko, *Nuclear Physics B* **91**, 210 (2001).

Acknowledgment

This research was made possible by the dedicated accelerator operational support at both LANL and FNAL. Funding support for P-25 work from the DOE Office of Nuclear Physics and the LANL LDRD program is gratefully acknowledged.

For more information, contact Bill Louis at 505-667-6723, louis@lanl.gov.

The Electric Dipole Moment of the Neutron

S.K. Lamoreaux (P-23), representing the EDM collaboration

We have a general notion of the meaning of the term "symmetry" particularly in regard to art and biology. In biological systems, symmetry at the molecular level has been known since 1848 when Pasteur discovered that tartaric acid could exist in two forms (e.g., "left-handed" and "right-handed," referred to as stereoisomers) that are mirror images of each other. Both forms are produced in inorganic processes, whereas only one-handedness is produced by or is useful to natural organic processes. The very fact that molecules can exist with either handedness implies that the atomic constituents are themselves very highly symmetric. This is expected because the electrostatic interaction that binds electrons in atoms does not distinguish between left and right.

In 1949, Norman Ramsey and Ed Purcell questioned the character of the nuclear force, in particular, whether it "conserved parity symmetry," P, which is to ask whether the force is the same if viewed as a mirror image (e.g., if left and right are important). They concluded that lack of P conservation would imply the possible existence of an EDM of the neutron. Shortly after, P asymmetry was observed in radioactive decay and subsequent theoretical work showed that a neutron EDM (nEDM) would require the existence of time reversal (T) asymmetry in addition to P asymmetry. As in the case of the question of P symmetry, in our daily lives we know that just as there is a distinction between left and right, there is a distinction between time moving forward and backward. If we drop a glass object on the floor and see it shatter, we do not expect to see the pieces subsequently come back together and the

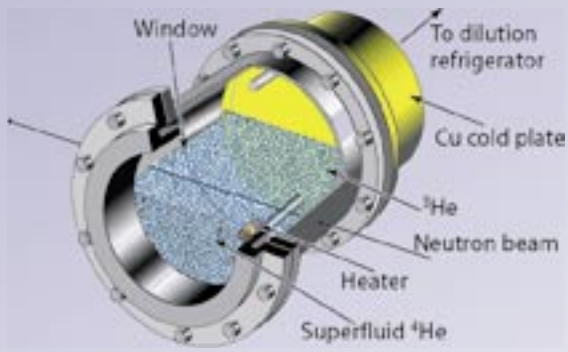

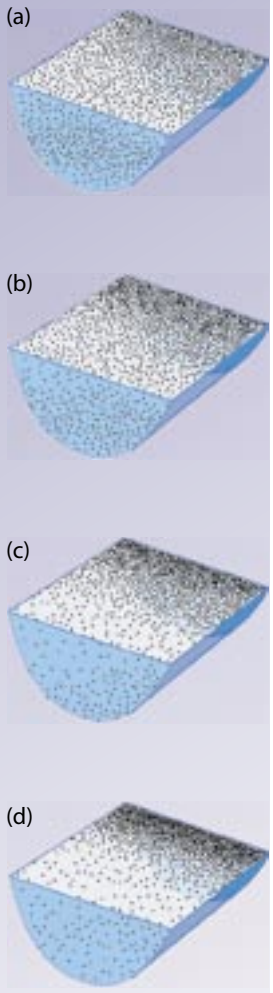

Figure 1. A three-dimensional rendering of the apparatus used to measure the diffusion and distribution of ^{3}He (dots) in superfluid ^{4}He (blue liquid in the bottom half of the cryostat cylinder). The window at the near end of the cylindrical cryostat is normally covered by a PMT, which is used to detect the scintillation light. The neutron beam enters from the right. The horizontal cryostat is mounted on a motion-controlled frame that allows it to be moved in two dimensions transverse to the beam. The effects of increasing heater power on the ^{3}He distribution in the cell are shown in the panels along the right side [Figure 1(a) through (d)]. In each case, the ^{3}He (dots) rapidly migrates away from the heater and towards the end of the cryostat connected to the dilution refrigerator. Figure 1(a) through (d) shows that the migration becomes more pronounced as the heater is set to 1, 2, 3, and 10 (arbitrary) heat units, respectively.

object jump back into our hand. However, nothing in the microscopic interactions that describe the object, its falling, and its subsequent shattering precludes this possibility. In this case, the direction of time we perceive is because such odd behavior is so improbable as to be impossible. As of 1964, it was assumed that the fundamental interactions governing the microscopic behavior of matter were time-reversal symmetric and that the flow of time in the universe was due to statistics as in the case of the shattering glass.

In 1964, T asymmetry, in addition to P asymmetry, in a fundamental interaction was (indirectly) observed in the decay of the "strange" K_0 meson. This again opened the possibility of an nEDM, and experimental limits on the possible size of the nEDM have been crucial in establishing the veracity of theories put forward to explain K_0 decay. The continuously improving nEDM experiments, with sensitivity increased by 9 orders of magnitude since 1950, have ruled out more theories than any other set of experiments in the history of physics. At the present level of EDM experiments, theoretical extensions to the so-called Standard Model, such as "supersymmetry," are being stringently tested.

The nEDM

A neutron has three quarks, a net charge of zero, and a magnetic moment. An nEDM would be evidence that the charge distribution of the internal quark constituents of the neutron is displaced relative to the center of mass. This displacement must lie along the neutron spin along with the magnetic moment.[1]

The usual technique employed for measuring the nEDM is magnetic resonance. When a polarized neutron is placed in parallel electric and magnetic fields, the spin precesses at the Larmor frequency (modified by the electric-field term)

$$f = \gamma B \pm 2dE, \qquad (1)$$

where γ = 3 Hz/mG (milli-Gauss) is the neutron gyromagnetic ratio, B is the applied magnetic field (typically, 10 mG or less), d is the nEDM usually expressed in "electron-centimeters" ($e$cm), and E is the applied electric field (typically 10 kV/cm)—the factor two in the second term results from the fundamental definition of the EDM. Under T reversal, the sign of B changes relative to E. We can produce this reversal in the laboratory by reversing E; a change in precession frequency with this reversal would be a direct detection of T asymmetry. The figure of merit, F, for an nEDM experiment is

$$F = E\sqrt{N\tau}, \qquad (2)$$

where E is the applied electric field, N is the number of neutrons measured per measurement cycle, and τ is the coherence time of the spin precession. The present best limit for the nEDM results from an experiment that employs spin-polarized UCNs stored for about 100 s in a 10 kV/cm electric field.[2]

UCNs are neutrons with kinetic energy so low they can be reflected from material surfaces for all angles of incidence. The energy of a UCN ($< 300 \times 10^{-9}$ eV) corresponds to a velocity of less than 7 m/s (just about the speed required for a four-minute mile!) and an effective temperature of 0.005 K.[3] UCNs can be stored in "bottles" for times approaching the β-decay lifetime of the neutron (~ 900 s).

Because the neutron precession frequency depends on the value of the magnetic field (see Equation 1), a spurious magnetic field associated with application of the electric field (caused by leakage currents, for example) can create a "false" or systematic EDM signal. To account for this possibility, the most recent experiment employs a "co-magnetometer" based on a dilute spin-polarized ^{199}Hg gas that fills the UCN storage vessel and is detected optically.

The results of this work limit the nEDM to $d < 5 \times 10^{-26}$ $e$cm. To understand the smallness of this limit, if the neutron were enlarged to the size of the earth, the displacement of the charge would correspond to about one wavelength of visible light.

An nEDM Experiment in Superfluid ^{4}He

For the experiment described in Reference 2, the UCN density was limited to 50/cm^3. More effective "superthermal processes" of producing UCNs are now under study at LANL.[4] In a superthermal source, relatively high-energy neutrons with an effective temperature of 10 K to 100 K (as a result of conventional moderation) inelastically scatter to lower energy in a material and become UCNs. If the scattering material is in a UCN storage bottle, the UCNs are trapped (the incoming high-energy neutrons easily penetrate the bottle). If the scattering material is at a very low temperature, the inverse process of inelastic scattering to high energy is impossible. Furthermore, if the material has low neutron absorption, the density of UCN builds

up until the rate of production equals the rate of loss due to β-decay and unavoidable losses on the storage-bottle surfaces. Two effective superthermal converters are superfluid ^{4}He and solidified deuterium gas. Superfluid ^{4}He is a nearly perfect superthermal converter because it has no nuclear absorption. We anticipate that we can obtain a UCN density of over 500/cm^3; we demonstrated the basic technology at the LANSCE in December 2001. We are proposing a new type of nEDM experiment based on this technology[1,5] and expect a possible factor of 100 improvement in the experimental limit, because we anticipate

- a factor of 5 increase in the electric field because of the good dielectric properties of superfluid helium,
- a factor of 100 increase in the number of stored UCNs, and
- a factor of 5 increase in the spin coherence time.

Using Equation 2 above, this implies a factor of about a 100 increase in the figure of merit.

^{3}He Magnetometry

The only substance that can dissolve and remain in solution in superfluid ^{4}He at low temperatures is the rare isotope ^{3}He. ^{3}He has an intrinsic nuclear spin of one-half and a magnetic moment. Furthermore, it is expected to have an extremely small EDM because of shielding by the atomic electrons. ^{3}He can be polarized and dissolved in superfluid ^{4}He, and we are presently studying the possibility of using it for a co-magnetometer in a superfluid ^{4}He nEDM experiment.

It is well-known that ^{3}He absorbs neutrons readily, with the reaction yielding a proton, a triton, and 764 keV of kinetic energy. The energy released by this reaction creates scintillation light in superfluid helium, and the fact that such a reaction occurred can be readily detected. Furthermore, the reaction is spin-dependent; when the ^{3}He and UCN spins are parallel, there is no reaction, but if the spins are oppositely directed, the reaction rate is twice the unpolarized rate.

If the UCN and ^{3}He spin polarization are perpendicular to the applied magnetic field, they will precess at their respective Larmor frequencies, which are the same to within 10% because the gyromagnetic ratios are equal to within 10%. The spin polarizations will oscillate between being parallel and antiparallel, and the scintillation light will be modulated at 10% of the Larmor precession frequency. A change in this frequency with a change in the electric field orientation would be evidence for an nEDM.

Because the ^{3}He-UCN relative precession rate is sensitive to the static magnetic field, our experiment still needs a co-magnetometer. In practice, monitoring the field external to the UCN storage volume does not provide an adequate measure of systematic magnetic fields (e.g., due to leakage currents) seen by the UCN.[1,2] Our current plan is to use SQUID sensors to directly monitor the ^{3}He precession to provide a measurement of the time- and volume-average magnetic field seen by both the ^{3}He atoms and the UCN while they are being stored together. SQUID sensors being studied by P-21 have enough sensitivity to measure the magnetic fields from a functioning brain and therefore will have sufficient sensitivity to detect the magnetic field from the population of precessing ^{3}He atoms as proposed in the EDM experiment. Experiments at LANL have focused on proving that SQUID sensors will perform in the environment of the proposed EDM experiment.[5,6]

The Diffusion of ^{3}He Atoms in Superfluid Helium

For ^{3}He atoms to be effective as a co-magnetometer, they must uniformly sample the UCN storage bottle. We predicted that the diffusion rate should be proportional to the temperature to the inverse-seventh power. Using the scintillation light from the ^{3}He neutron-capture reaction, we were able to perform tomography on a cylindrical cell 50 mm in diameter and 50 mm long. We used the cold neutron beam on flight path 11A (located at the Lujan Center at LANSCE), collimated to a

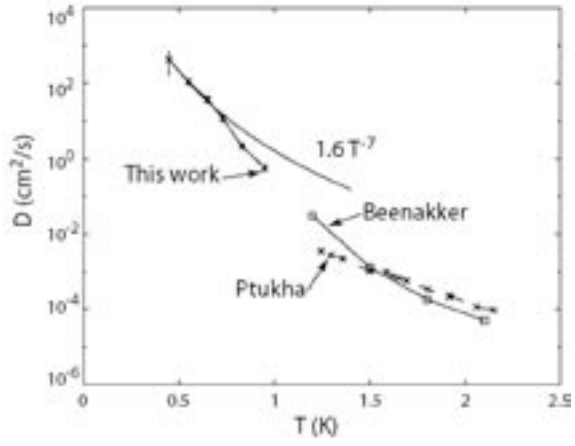

Figure 2. Our experimental results for the diffusion coefficient compared to previous measurements.

diameter of about 2 mm. The cell was mounted on a horizontal dilution refrigerator that could be cooled to 0.3 K. The entire refrigerator/cell cryostat assembly was mounted on a translation apparatus so that it could be moved relative to the fixed cold neutron beam. A three-dimensional rendering of the apparatus is shown in Figure 1. The integrated ^{3}He concentration along a path through the cell was determined by the scintillation rate. The subpanels in Figure 1(a) through (d) show the effects when a heater located near the side of the cell is turned on; the ^{3}He becomes more concentrated at the refrigerated end of the cell.

The results of our experimental measurements of the diffusion coefficient are shown in Figure 2. Our technique allowed extending the measurements from the previous lower limit of 1.2 K to a new lower limit of 0.4 K. Most importantly, we verified that the ^{3}He distribution is uniform (in the absence of a heat flux) and that the diffusion coefficient follows the T^{-7} prediction at temperatures below 0.7 K. These results were published along with an accompanying paper that provides a theoretical analysis of our results.[7]

Conclusion

We are developing a new experiment at LANL to improve the limit of the nEDM by over two orders of magnitude, and we expect to be producing data by 2008. Such an improved limit is crucial to our understanding of T asymmetry in fundamental interactions and has broad applications from elementary particle physics to our understanding of the matter-antimatter asymmetry in the universe.

References

1. I.B. Khriplovich and S.K. Lamoreaux, *CP Violation Without Strangeness* (Springer-Verlag, Heidelberg, 1997).
2. P.G. Harris, C.A. Baker, K. Green *et al.*, "New experimental limit on the electric dipole moment of the neutron," *Physical Review Letters* **82**(5), 904–907 (1999).
3. R. Golub, D.J. Richardson, and S.K. Lamoreaux, *Ultracold Neutrons* (Adam-Hilger, Bristol, 1991).
4. C.L. Morris, J.M. Anaya, T.J. Bowles *et al.*, "Measurements of ultracold-neutron lifetimes in solid deuterium," *Physical Review Letters* **89**(27), 272501 (2002).
5. M.A. Espy, A.N. Matlachov, R.H. Kraus, Jr. *et al.*, "SQUIDs as detectors in a new experiment to measure the neutron electric dipole moment," *IEEE Transactions on Applied Superconductivity* **9**(2), 3696–3699 (1999).
6. M.A. Espy, A.N. Matlashov, R.H. Kraus, Jr., *et al.*, "The temperature dependence of SQUID noise at temperatures below 4 K," *Physica C* **368**, 185–190 (2002).
7. S.K. Lamoreaux, G. Archibald, P.D. Barnes *et al.*, "Measurement of the ^{3}He mass diffusion coeffiecient in superfluid ^{4}He over the 0.45–0.95 K temperature range," *Europhysics Letters* **58**, 718–724 (2002).

Acknowledgment

This work is supported by the LANL LDRD program.

For more information, contact Steve Lamoreaux at 505-665-1768, lamore@lanl.gov, or visit the EDM web page at http://p25ext.lanl.gov/edm/edm.html (which includes a complete list of the experiment's collaborators).

The NPDGamma Experiment

J.D. Bowman, M. Gericke, G.S. Mitchell, S.I. Penttilä, G. Peralta, P-N. Seo, W.S. Wilburn (P-23), representing the NPDGamma collaboration

The nature of weak interactions between strongly interacting hadrons is not well understood. The NPDGamma ($\vec{n} + p \rightarrow d + \gamma$) experiment,[1] currently under construction at the LANSCE, will study the parity-violating weak interaction between the most common hadrons, protons, and neutrons. The hadronic weak interaction is observed in nuclei and nuclear processes,[2] but interpretation of these experiments is difficult because of the complicated many-body dynamics of a nucleus. The goal of the NPDGamma experiment is to measure the parity-violating directional gamma-ray asymmetry in the reaction $\vec{n} + p \rightarrow d + \gamma$ to an accuracy of 5×10^{-9}, which is approximately 10% of its predicted value.[3,4] Such a result, in a simple system, will provide a theoretically clean measurement of the weak pion-nucleon coupling, thus resolving the long-standing nuclear-physics controversy over its value.

Theory Background

The flavor-conserving weak interaction between hadrons is the most poorly tested aspect of electroweak theory.[4] While much is known about quark-quark weak interactions at high energies, the low-energy weak interactions of hadrons (particles made of quarks, such as the nucleons—the proton and the neutron) are not well measured. At low energies, the effects of the weak interaction are typically obscured by other processes, making their experimental study challenging. In terms of the meson-exchange picture of the weak nucleon-nucleon interaction,[4] the weak-pion exchange is particularly interesting because it is the longest-range component of the interaction and is therefore presumably the most reliably calculable. The hadronic exchange of neutral currents, which is expected to dominate the weak-pion exchange between nucleons, has not been isolated experimentally in an unambiguous way. For both of these reasons, the coupling constant, H_π^1, for pion exchange in the weak nucleon-nucleon interaction is of special interest.

An accurate measurement of H_π^1 in a simple nucleon-nucleon system is needed to resolve previous experimental inconsistencies. A two-nucleon system, such as in the $\vec{n} + p \rightarrow d + \gamma$ process, is sufficiently simple that the measured asymmetry of the emitted gamma rays can be related to the weak meson-nucleon-nucleon coupling with negligible uncertainty to nuclear structure. The relationship between the parity-violating asymmetry A_γ and H_π^1 (where A_γ is the correlation between the direction of emission of the gamma ray and the neutron polarization) is calculated to be $A_\gamma \approx -0.045\ H_\pi^1$. The goal of NPDGamma is to measure A_γ to a precision of $\pm 5 \times 10^{-9}$, which will determine H_π^1 to $\pm 1 \times 10^{-7}$. Such a result will clearly distinguish between the values for H_π^1 extracted from experiments in nuclear systems and between predictions by various theories of the weak interaction of hadrons in the nonperturbative QCD regime.

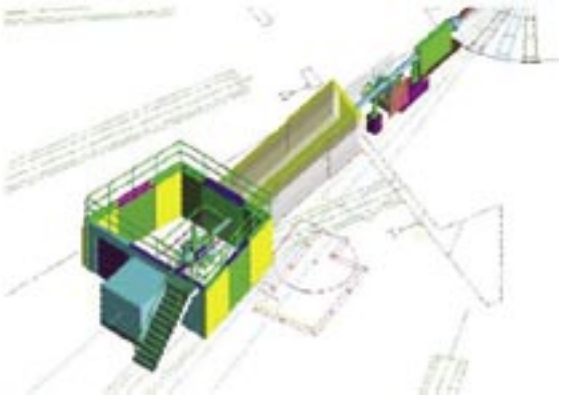

Figure 1. Depiction of FP12 at the Lujan Center at LANSCE. Construction of the flight path and the experimental cave is essentially complete. Commissioning of the flight path and the experimental apparatus will begin in January 2004.

NPDGamma Experiment

To determine H_{π}^{1} with an uncertainty of 1×10^{-7}, we must achieve a statistical uncertainty of 0.5×10^{-8} on A_{γ}. This means that the experiment must detect a few $\times 10^{17}$ of the 2.2-MeV gamma-rays from the $\vec{n} + p \rightarrow d + \gamma$ reaction. In addition, possible systematic errors in the experiment require careful attention. The tiny parity-violating signal in the reaction will be isolated by flipping the neutron spin. The real asymmetry will change sign under spin reversal, while spin-independent false asymmetries will not. The weak interaction is the only fundamental-particle interaction that can produce a parity-violating signal; parity violation is simply described as a difference between a physical process and its mirror image. For example, in the $\vec{n} + p \rightarrow d + \gamma$ reaction, if more gamma rays are emitted in the same direction as the neutron spin, rather than in the opposite direction, then that is a parity-violating signal and must be caused by the weak interaction. The experiment then consists of observing the direction of emission of the gamma rays from many $\vec{n} + p \rightarrow d + \gamma$ captures, and if there is an asymmetry in their distribution with respect to the neutron-polarization direction, the effect of H_{π}^{1} has been observed.

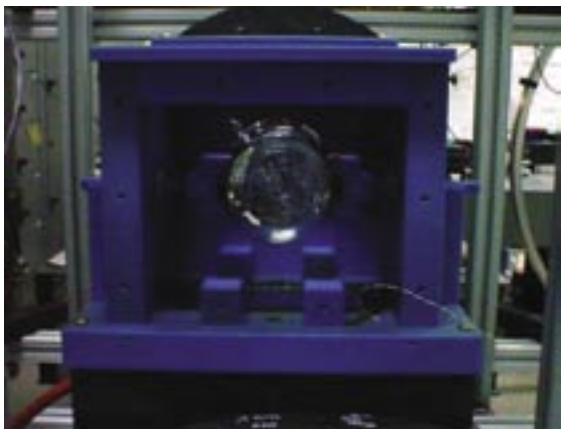

Figure 2. The ^{3}He spin filter used to polarize the neutron beam. The glass cell is 11 cm in diameter and contains ^{3}He and rubidium. A laser is used to polarize the rubidium atoms, which then transfer their polarization to the ^{3}He nuclei. The blue structure is used to support the glass cell and to provide an environment where it can be kept at a warm temperature (150°C) to produce rubidium vapor.

The requirements for the experiment are a large number of polarized, cold neutrons; a method of flipping the neutron polarization; a proton target; and a detector system for the 2.2-MeV gamma rays. The experiment consists of a pulsed, cold neutron beam, transversely polarized by transmission through polarized ^{3}He, with polarization reversal achieved on a pulse-by-pulse basis by an rf spin flipper. The neutrons are incident on a liquid parahydrogen target. The 2.2-MeV gamma rays from the capture reaction will be detected by an array of cesium-iodide scintillators coupled to vacuum photodiodes and operated in current mode.

Cold Neutron Beam and Polarizer

The experiment requires a high flux of cold neutrons with energies below 15 meV. Although such neutrons are available from cold moderators at both reactors and spallation neutron sources, the nature of the neutron flux from a pulsed spallation source provides a very powerful diagnostic tool for a number of possible systematic effects for this experiment. At LANSCE, the cold neutron source consists of a liquid-hydrogen moderator coupled to the 20-Hz pulsed neutron source. At cold-neutron energies, it is possible to use neutron guides to transport neutrons. Just as a difference in the indices of refraction will cause total internal reflection of light incident at shallow angles on the interface between two media, magnetic properties of the surface of a neutron guide can be used to reflect neutrons incident at glancing angles (below a well-known critical angle) on the guide surface. The function of the neutron guide is to conserve the high cold-neutron flux available near the moderator.

For the experiment, a new beam line and neutron guide, flight path 12 (FP12), have been built at the Lujan Center.[5] A drawing of the FP12 layout with the experimental cave at its end is shown in Figure 1. To observe parity violation (in the distribution of gamma rays with respect to the neutron-polarization direction), the experiment requires polarized neutrons. Cold neutron beams can be polarized in several ways, but the best technology for NPDGamma is a ^{3}He spin filter.[6] ^{3}He spin filters (Figure 2) are compact, possess a

large phase-space acceptance, produce a negligible fraction of capture gamma-ray background, and do not require strong magnetic fields or produce field gradients. This is important for the control of systematic errors in the experiment. The thickness of the spin filter can be optimized for polarization versus transmission.

Neutron Spin Flipper

For NPDGamma, the neutron spins are flipped on a 20-Hz pulse-by-pulse basis with an rf spin rotator, or spin flipper (RFSF). The RFSF is a shielded solenoid that operates according to the well-known principles of nuclear magnetic resonance. In the presence of a homogeneous constant magnetic field and an oscillating magnetic field in a perpendicular direction, the neutron spin will precess, and the amplitude of the oscillating field can be selected to precess the spin by 180° as the neutron travels through the spin-flipper volume. The spin flip is introduced on a pulse-by-pulse basis by simply turning the rf field on and off. The solenoid produces only negligible external magnetic fields and field gradients—an important property given the possible sensitivity of the detector apparatus to magnetic-field-induced gain shifts.

Proton Target

In the liquid-hydrogen (proton) target, it is essential that the polarized neutrons retain their polarization until they are captured. Many of the neutrons will scatter in the target before they are captured, and the spin dependence of the scattering is therefore important. The ground state of the hydrogen molecule (known as parahydrogen) has spin of zero (J=L=S=0), and the first excited state, the lowest orthohydrogen state, is at 15 meV above the parastate. A large fraction of the cold neutrons possess energies lower than 15 meV. Because these neutrons cannot excite the parahydrogen molecule into its first excited state, only elastic scattering and capture are allowed, and spin-flip scattering is forbidden. The neutron polarization therefore survives the scattering events that occur before the capture. Higher-energy neutrons will undergo spin-flip scattering and therefore lose their polarization. The liquid-hydrogen target must be in the parastate. For liquid hydrogen held at 20 K and atmospheric pressure, the equilibrium concentration of parahydrogen is 99.8%, which is low enough to ensure a negligible population of orthohydrogen.

Figure 3. The gamma-ray detector array includes 48 cesium-iodide crystals. The housings of 16 of the crystals are visible in the photo. The effect of the hadronic weak interaction is measured as an asymmetry in the event rate between the upper and lower detector hemispheres. The RFSF is mounted on the left side of the array.

Cesium-Iodide Gamma-Ray Detector Array

Finally, the experiment must detect the 2.2-MeV gamma rays from the neutron capture. Given the small size of the expected asymmetry and the goal precision of the experiment, the number of events required to achieve sufficient statistical accuracy in a reasonable time immediately leads to the conclusion that the 2.2-MeV gamma rays must be counted in current mode. This means that instead of observing individual events in the detector, many are seen at once, and the sum of their presence is detected as a total voltage or current from the detector electronics rather than as individual pulses. It is important to demonstrate in a current-mode measurement that the electronic noise is negligible compared to the shot noise because of

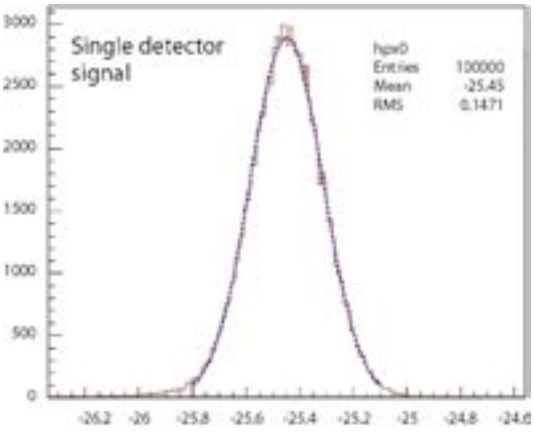

Figure 4. A histogram of a detector signal, measuring the electronic noise. The width of the distribution is of order 0.1 mV, which corresponds to the theoretical limit due to preamplifier Johnson noise of 20 fA/√Hz . This will allow the current-mode detectors to take data at the counting-statistics limit and to quickly demonstrate that no false asymmetry effects are observed in the electronics and data-acquisition system.

the discrete nature of the energy deposited by each gamma ray and the number of photoelectrons produced by each event. In addition, the detector must cover a large solid angle with a large, time-independent efficiency that is unaffected by neutron spin reversal and radiation damage. Segmentation of the detector is required to resolve the angular dependence of the expected parity-violating signal and to discriminate false effects. A photo of the fully constructed detector array of 48 cesium-iodide scintillator crystals is shown in Figure 3. The noise performance of the detectors and their preamplifier electronics has been measured in the laboratory, and it corresponds well to predictions based on the fundamental limit of Johnson noise. (A histogram of a single detector signal is shown in Figure 4, and the width of the distribution is a measure of the noise in the electronics.) This will allow the detectors to accumulate data at the counting statistics limit and to quickly demonstrate that no false experimental effects exist in the electronics.

Conclusion

A sensitive measurement of the parity-violating gamma asymmetry in the reaction $\vec{n} + p \rightarrow d + \gamma$ can give definitive information on one of the most important and interesting components of the weak nucleon-nucleon interaction. Engineering runs have demonstrated the performance of the essential components of the experiment; this includes published results for the FP12 moderator performance and measurements of parity-violating asymmetries in neutron capture on nuclear targets (chlorine, cadmium, and lanthanum) to a precision of 6×10^{-6}—limited only by counting statistics. Construction of the detector array is complete and laboratory tests indicate that noise levels of the electronics are close to the theoretical limits and thus allow the measurement of asymmetries at the level of a few parts per billion. The experimental design incorporates a number of powerful diagnostics to isolate systematic effects. Commissioning of the final construction of the experiment will begin in early 2004, and data taking will commence in late 2004. The NPDGamma experiment to search for the parity-violating gamma asymmetry in the reaction $\vec{n} + p \rightarrow d + \gamma$ will achieve a sensitivity that is likely to obtain a nonzero result, providing an experimental and unambiguous measure of the hadronic weak interaction in a simple and calculable system.

References

1. W.M. Snow, A. Bazhenov, C.S. Blessinger *et al.*, "Measurement of the parity violating asymmetry A_γ in $\vec{n} + p \rightarrow d + \gamma$," *Nuclear Instruments and Methods A* **440**(3), 729–735 (2000).
2. G.E. Mitchell, J.D. Bowman, S.I. Penttila *et al.*, "Parity violation in compound nuclei: Experimental methods and recent results," *Physics Reports* **354**(3), 157–241 (2001).
3. B. Desplanques, J.F. Donoghue, and B.R. Holstein, "Unified treatment of the parity-violating nuclear force," *Annals of Physics* **124**, 449–495 (1980).
4. E.G. Adelberger and W.C. Haxton, "Parity violation in the nucleon-nucleon interaction," *Annual Review of Nuclear and Particle Science* **35**, 501–558 (1985).
5. The brightness of the FP12 moderator has been measured by the NPDGamma collaboration. The peak brightness is 1.25×10^8 neutrons/cm^2/s/sr/meV/μA at 3.3 meV. (P.-N. Seo *et al.*, submitted in 2003 to *Nuclear Instruments and Methods A*).
6. G.L. Jones, T.R. Gentile, A.K. Thompson *et al.*, "Test of ^{3}He-based neutron polarizers at NIST," *Nuclear Instruments and Methods A* **440**(3), 772–776 (2000); D.R. Rich, J.D. Bowman, B.E. Crawford *et al.*, "A measurement of the absolute neutron beam polarization produced by an optically pumped ^{3}He neutron spin filter," *Nuclear Instruments and Methods A* **481**, 431–453 (2002).

Acknowledgment

Assistance in the construction and design of this experiment has been provided by LANSCE-12 and LANSCE-3. This work was supported in part by the DOE Office of Energy Research (Contract W-7405-ENG-36), the National Science Foundation (Grant No. PHY-0100348), and the Natural Sciences and Engineering Research Council of Canada.

For further information, contact Gregory Mitchell at 505-665-8484, gmitchell@lanl.gov.

Extreme Astrophysics—The High-Resolution Fly's Eye Experiment

C. Sinnis, C.M. Hoffman, M.H. Holzscheiter, C.A. Painter (P-23), J.F. Amann, M.D. Cooper, L.J. Marek, T.N. Thompson, D. Tupa (P-25), J.S. Sarracino (X-5), R.U. Abbasi, T. Abu-Zayyad, G. Archbold, K. Belov, Z. Cao, H. Dai, A.A. Everett, J.H.V. Girard, R.C. Gray, W.F. Hanlon, P. Huntemeyer, B.F. Jones, C.C.H. Jui, D.B. Keida, K. Kim, E.C. Loh, K. Martens, J.N. Matthews, J.R. Meyer, S.A. Moore, P. Morrison, A.N. Moosman, J.R. Mumford, K. Reil, R. Riehle, P. Shen, J.D. Smith, P. Sokolsky, R.W. Springer, B.T. Stokes, S.B. Thomas, L.R. Wiencke, T.D. VanderVeen (University of Utah), J.A. Bellido, R.W. Clay, B.R. Dawson, K.M. Simpson (University of Adelaide, Australia), J.W. Blez, M.A. Kirn, M.W. Munro (University of Montana), D.R. Bergman, L. Perera, S.R. Schnetzer, G.B. Thomson, A. Zech (Rutgers University), J. Boyer, B. Knapp, E. Mannel, M. Seman, C. Song, S. Westerhoff, X. Zhang (Columbia University), N. Mango, M. Sasaki (University of Tokyo, Japan), G. Martin, J.A.J. Matthews, M. Roberts (University of New Mexico)

The earth is constantly bombarded by high-energy particles of unknown origin. These particles, known as cosmic rays, have energies up to and beyond 10^{20} eV (10^{20} eV = 16 J, which is nearly the energy packed into a major league fastball). These are the highest energy particles in the universe. Their origin is unknown, and they represent one of the mysteries of modern science. What are they? How do they attain their enormous energies? How do they propagate to earth? Compounding the inherent difficulty of studying extraterrestrial particles is the rarity of these ultra-high-energy cosmic rays. Above 10^{20} eV, only one of these particles will pass through a square kilometer of the earth in a century. Figure 1 shows the cosmic-ray spectrum from 1 GeV (i.e., a billion electron-volts to above 10^{20} eV). The HiRes experiment located in Dugway, Utah, seeks to gain an understanding of the properties of these particles: how many there are, where they come from, and what they are.

The HiRes Experiment

When a UHECR enters the atmosphere, it interacts with the molecules in the air, creating an EAS. The EAS is composed of billions of particles (electron, positrons, gamma rays, and muons) traveling at the speed of light towards the earth. The passage of the charged particles excites nitrogen molecules in the air. These excited molecules emit fluorescence light. Because this light is emitted isotropically, a detector does not need to be "in the beam" to be detected—therefore, a relatively small detector with an enormous aperture will do the job. The HiRes detector consists of two independent sites separated by 12.6 km so that each event may be viewed stereoscopically. This stereoscopic view gives the detector depth perception and allows us to measure the distance to each event. At each site, there is a set of 5-m^2 mirrors, each equipped with a 256-PMT camera placed in the focal plane. Each PMT has a 1° field of view. The HiRes I site has 21 mirrors covering an elevation range from 3° to 17°, and the HiRes II site has 44 mirrors covering an elevation range from 3° to 31°. Both sites provide a 2-π azimuthal coverage of the sky. The aperture of the full HiRes detector is 10,000 km^2 sr at 10^{20} eV. In HiRes I, the shower images are stored in sample-and-hold electronics with a 5.6-μs window; in HiRes II, the information is digitized with a 10-MHz flash (analog-to-digital converter) system. The air-fluorescence technique (Figure 2) used in our experiments allows us to detect the passage of an air shower with the HiRes instrument. The entire longitudinal development of the air shower is obtained by recording the amount of light detected in each PMT.

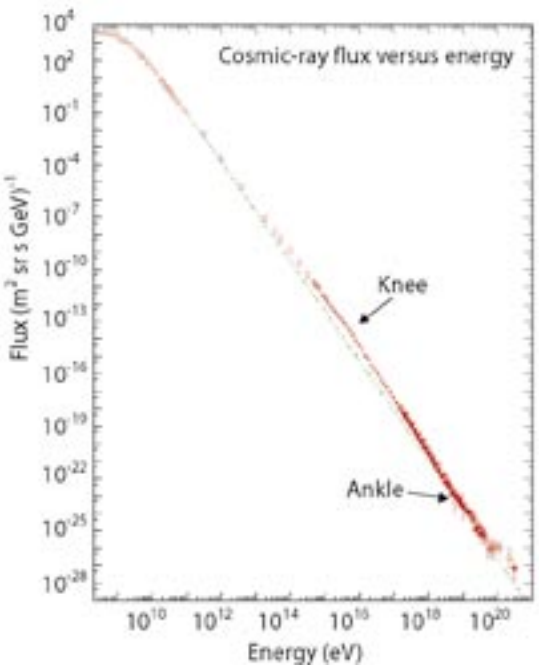

Figure 1. The cosmic-ray spectrum from 1 GeV to 10^{20} eV. The spectrum is well represented by a power law but with two features. At an energy of roughly 10^{15} eV, the spectrum begins to fall faster with energy (which is the knee of the cosmic-ray spectrum), and at an energy of roughly $10^{18.5}$ eV, the spectrum hardens slightly (which is the ankle of the cosmic-ray spectrum). Above 10^{20} eV, the flux is about one particle per square kilometer per century.

UHECR Science

A UHECR flux above an energy of 6 x 10^{19} eV is of fundamental importance in astrophysics studies. Protons with energies in excess of this will interact with microwave background radiation and lose energy through pion production—this process is known as the GZK effect (for Greisen, Zatsepin, and Kuzmin, the co-discoverers of the effect).[1,2] The mean-free path for this interaction is roughly 20 million light years; therefore, the flux of particles above this energy is expected to fall rapidly—unless the "point" sources of these particles are relatively close to the earth. If the point sources *are* close to the earth, the particles should point back to them because at these energies the particles bend via intergalactic magnetic fields at relatively small (< 2°) angles. However, the particles that we detected to date do not appear to point back to any objects capable of accelerating particles to these energies.[3]

At present, there is disagreement between the only two experiments that have measured the flux at these energies—the HiRes and the Akeno Giant Air Shower Array (AGASA). The AGASA is a traditional scintillator array composed of 111 particle detectors spread over 100 km^2. Figure 3 shows the present status of the world's dataset.[4] The curve on the figure is what one would expect if the sources of UHECRs were uniformly distributed throughout the universe and if the GZK effect were included. (The data from HiRes and AGASA are indicated in the legend.) Although the HiRes data are consistent with this curve, the AGASA data are not. The overall offset of the two datasets is due to systematic uncertainties in the absolute energy scale of the two experiments. The HiRes data were taken in "monocular" mode—determining the distance to the air shower (and therefore the energy of the primary cosmic ray) is not made directly but relies instead on a fit to the shower profile. At present, neither experiment has the statistical power or an understanding of systematic effects to make a definitive statement on the existence of the GZK effect.

If the GZK effect is not present, then there are many possible explanations, most of which involve exciting new physics. The solutions can be grouped into either a "top-down" or a "bottom-up" scenario. In the top-down scenario, the particles are the decay products of very massive particles, possibly relics left from the Big Bang.[5,6] In the bottom-up scenario, the particles are accelerated to high energies by astrophysical sources such as gamma-ray bursts or active galactic nuclei. In these scenarios, super-GZK events can be caused by a suppression of the proton-photon interaction at high energies, which would clearly violate Lorentz invariance and may be a signal of quantum gravity.[7,8] The super-GZK events may also be caused by the existence of a new strongly interacting particle (for example, a massive, stable hadron) that does not suffer from the energy loss in the 3-K radiation field.[9,10] Moreover, there may be unseen "local" astrophysical sources of UHECRs or ultra-high-energy neutrinos that may propagate over cosmological distances and interact with (massive) relic neutrinos within 160 million light years of the earth. If the latter were the case, a cascade of gamma rays and hadronic particles (known as the "Z-burst" model) would be detected.[11]

Each of the scenarios described above make different predictions as to the nature of UHECRs—are they protons, gamma rays, heavy nuclei, neutrinos, or some as yet undiscovered particle? Each of these particles is expected to have a different cross section; therefore, they will interact at different depths in the atmosphere, and the resulting air shower will have a different altitude of maximum development. Because the HiRes experiments observe the entire longitudinal development of the air shower, we can measure the altitude of the maximum shower with a resolution of roughly 30 g/cm^2. Although shower-to-shower

fluctuations preclude us from measuring the particle type on an event-by-event basis, we can determine the average composition of the UHECRs using the air-fluorescence technique. Finally, we want to know where these UHECRs are coming from. Do they come from point sources (if so, which objects are accelerating particles to such high energies) or are they isotropic? There is preliminary evidence from AGASA that the UHECRs come in clusters. If this claim is correct, it would imply that there are numerous stable sources of UHECRs. With an angular resolution of 0.4°, HiRes can verify or repudiate this claim.

Conclusion

Because the GZK effect is predicted to occur at a well-defined energy, knowing the true energy of each event is critical. Systematic errors must therefore be of the same order or smaller than statistical errors. The systematic errors in the current HiRes analysis are caused by a 10% uncertainty in the absolute fluorescence yield and by the attenuation of particles as they are absorbed in the atmosphere. To reduce the errors from atmospheric absorption, we have installed a set of lasers that allow us to continuously monitor the atmosphere over the entire aperture of the detectors. With these lasers, we can make atmospheric corrections on an event-by-event basis and calculate the aperture of the experiment on an hourly timescale. Most importantly, because HiRes was built to view all events stereoscopically, we can determine the shower distance and inclination angle from purely geometrical considerations. Figure 4 shows the stereo reconstruction of a typical event. Once the geometry of the shower is known, crosschecks can be performed on the atmospheric attenuation (because the two detector sites are, in general, a different distance from the shower). Such a crosscheck will allow us to better measure and control systematic uncertainties. A complete stereo analysis is now under way. Within five years of taking data, HiRes will detect 50 events with energies in excess of 6 x 10^{19} eV and 20 events above 10^{20} eV if there is no GZK effect. With these results, we will be able to make a statistically significant measurement of the GZK effect. Within the next several years, HiRes will have solved a major riddle of modern physics—the nature of the highest-energy particles in the universe.

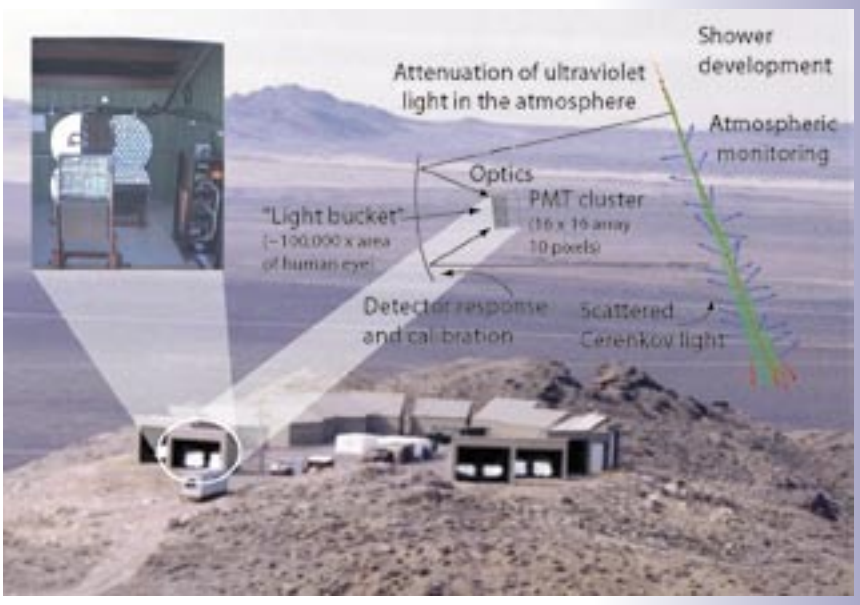

Figure 2. Schematic view of the detection of an EAS using the air-fluorescence technique. The electromagnetic particles in the air shower excite nitrogen molecules in the atmosphere, which radiate ultraviolet light. This light passes through the atmosphere (as much as 40 km) where it is absorbed and scattered. The surviving light is reflected from the mirrors and focused onto a fast camera composed of PMTs.

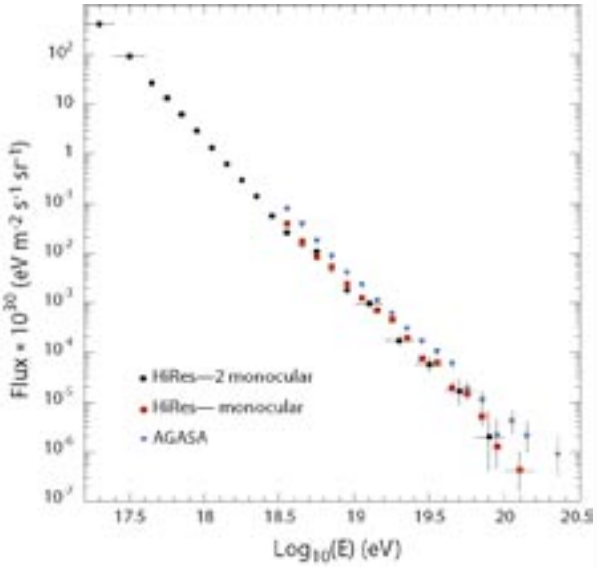

Figure 3. The UHECR as measured by HiRes in monocular mode and the AGASA experiment. The flux has been multiplied by E^3 to show the structure. The offset between the two experiments arises from systematic uncertainties in the absolute energy calibration of the two detectors. Although the HiRes data are consistent with the existence of the GZK effect, the AGASA data indicate that the spectrum hardens above 10^{20} eV.

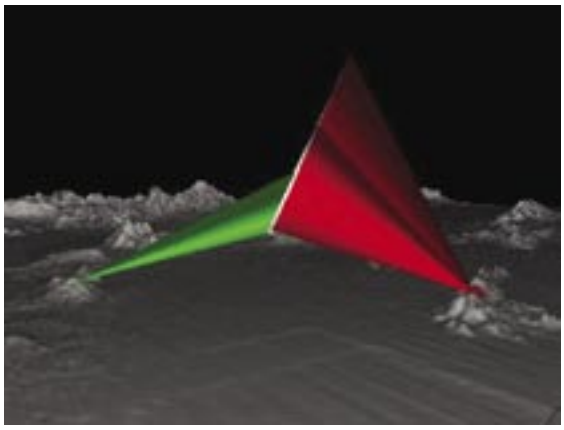

Figure 4. A typical event as seen by HiRes in stereo mode. Each detector determines a plane in which the shower lies. The intersection of the two planes determines the full three-dimensional geometry of the event.

References

1. K. Greisen, "End to the cosmic-ray spectrum," *Physical Review Letters* **16**(17), 748 (1966).
2. G.T. Zatsepin and V.A. Kuzmin, "Upper limit of spectrum of cosmic rays," *Journal of Experimental and Theoretical Physics* **4**(3), 78 (1966).
3. J.E. Elbert and P. Sommers, "In search of a source for the 320-EeV fly's eye cosmic ray," *Astrophysical Journal* **441,** 151 (1995).
4. T. Abu-Zayyad *et al.,* "Measurement of the flux of ultra-high-energy cosmic rays from monocular observations by the high resolution fly's eye experiment," submitted to *Physical Review Letters.*
5. P. Bhattacharjee, C.T. Hill, and D.N. Schramm, "Grand unified theories, topological defects, and ultrahigh-energy cosmic rays," *Physical Review Letters* **69,** 567 (1992).
6. C.T. Hill, D.N. Schramm, and T.P. Walker, "Ultrahigh-energy cosmic rays from superconducting cosmic strings," *Physical Review D* **36,** 1007 (1987).
7. S. Coleman and S.L. Glashow, "High-energy tests of Lorentz invariance," *Physical Review D* **59,** 151 (1999).
8. G. Amelino-Camelia and T. Piran, "Planck-scale deformation of Lorentz symmetry as a solution to the ultra-high-energy cosmic rays and the TeV-photon paradoxes," *Physical Review D* **64,** 036005 (2001).
9. G.R. Farrar, "Detecting light-gluino-containing hadrons," *Physical Review Letters* **76,** 4111 (1996).
10. I.F.M. Albuquerque, G.R. Farrar, and E.W. Kolb, "Exotic massive hadrons and ultra-high-energy cosmic rays," *Physical Review D* **59,** 015021 (1999).
11. T.J. Weiler, "Cosmic-ray neutrino annihilation on relic neutrinos revisited: A mechanism for generating air showers above the Greisen-Zatsepin-Kuzmin cutoff," *Astroparticle Physics* **11,** 303 (1999).

Acknowledgment

We gratefully acknowledge the contributions from the technical staffs of our home institutions and the Utah Center for High Performance Computing. The cooperation of Colonel E. Fischer and Colonel G. Harter of the U.S. Army Dugway Proving Grounds staff is greatly appreciated. This work is supported by grants from the National Science Foundation, including PHY-9321949, PHY-9974537, PHY-9904048, PHY-0071069, and PHY-0140688; by DOE grant FG03-92ER40732; and by the Australian Research Council.

For more information, contact Gus Sinnis at 505-665-6943, gus@lanl.gov.

Teravolt Astrophysics—The Milagro Gamma-Ray Observatory

C. Sinnis, B.L. Dingus, T.J. Haines, C.M. Hoffman, F.W. Samuelson (P-23), G.R. Gisler (X-2), R. Atkins, M.M. Gonzalez, J.E. McEnery, M.E. Wilson (University of Wisconsin), W. Benbow, D.G. Coyne, D.E. Dorfan, L.A. Kelley, M.F. Morales, D.A. Williams, S. Westerhoff (University of California, Santa Cruz), D. Berley, E. Blaufuss, J. Bussons, J.A. Goodman, E. Hays, C.P. Lansdell, D. Noyes, A.J. Smith, G.W. Sullivan (University of Maryland), T. DeYoung (University of California, Santa Cruz, and University of Maryland), R.W. Ellsworth (George Mason University), L. Fleysher, R. Fleysher, A.I. Mincer, P. Nemethy (New York University), J. Linnemann, X. Xu (Michigan State University), R.S. Miller, J.M. Ryan (University of New Hampshire), A. Shoup, G.B. Yodh (University of California, Irvine)

Milagro is a new type of astronomical telescope. Like conventional telescopes, Milagro is sensitive to light, but the similarities end there. Whereas "normal" astronomical telescopes view the universe in visible light, Milagro "sees" the universe at very high energies. The "light" that Milagro sees is about one trillion times more energetic than visible light. Although these particles of light, known as photons, are the same as the photons that make up visible light, they behave quite differently simply because they are much more energetic. Viewing the heavens in high-energy photons creates quite a different picture from what we see when we look up at the night sky. There are fewer objects, and they are much more extreme—in the visible, we detect mostly thermal processes and blackbody radiation.

When we view the universe in TeV gamma rays (1 TeV is one trillion electron volts; normal light has a few electron volts of energy), we detect non-thermal radiation and particle acceleration. The light sources that we detect contain super-massive black holes and neutron stars. Some of these sources are highly variable, flaring on a timescale of minutes to days. Until the advent of the Milagro Observatory, located at the LANL Fenton Hill site, there was no instrument capable of continuously monitoring the entire overhead sky in the TeV-energy regime. The existing instruments, known as air Cerenkov telescopes (ACTs), had to be pointed at small regions of the sky (usually at known sources) and could only look at a light source during the time of year that it is overhead at night. Even then, they could only look at the source if the weather was good and the moon was set. But Milagro is ideally suited to monitor the variable TeV universe and discover new sources of TeV gamma rays. With this instrument, we hope to discover new sources of TeV photons, to observe TeV emission from gamma-ray bursts, and to discover primordial black holes or some completely new phenomena.

Physics with Milagro

High-energy gamma-ray astronomy seeks to understand the most extreme environments in the universe and to use the beams of gamma rays from these distant sources to further our understanding of the fundamental laws of physics at energies not attainable in earth-bound experiments. The known sources of gamma rays include supernova remnants, super-massive black holes (known as active galactic nuclei, or AGN), and gamma-ray bursts (the most energetic phenomena in the universe). Gamma rays are also produced when high-energy cosmic rays interact with matter in our galaxy. Other potential sources include more exotic objects (which may or may not be detectable) such as "evaporating" primordial black holes, topological defects, and dark-matter particle annihilation and decay. The gamma rays from distant sources interact with the ambient fields in the universe as they travel to earth. By measuring the effects of these interactions, we can understand the nature of the fields that pervade the universe. Two particle-interaction effects are of concern to us—particle interactions with the intergalactic-infrared-radiation fields and those with the quantum fields that define the universe. The infrared-radiation field results from the formation of, and the nuclear-burning process in, stars and from the subsequent absorption and re-radiation of the energy produced in this process

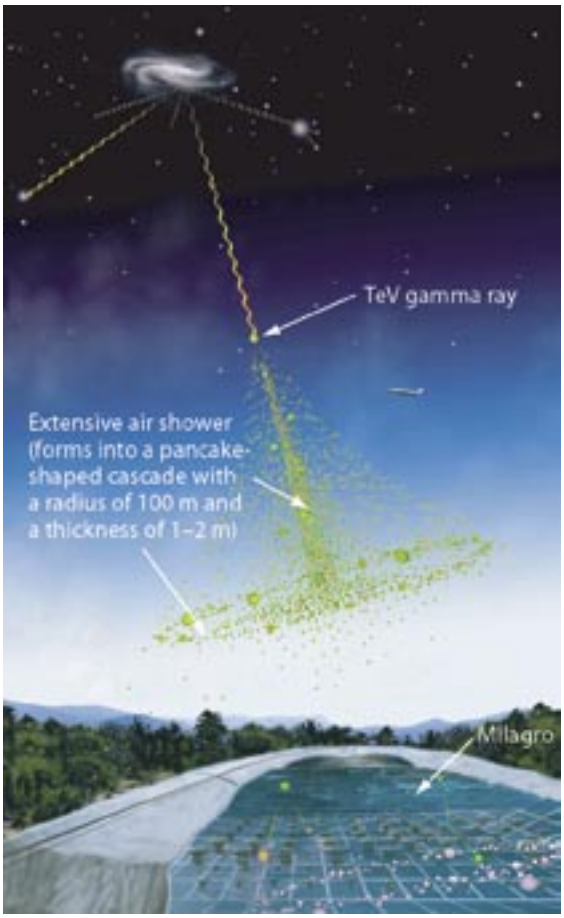

Figure 1. Rendering of Milagro. An astrophysical source emits TeV gamma rays, which propagate to earth. The gamma ray interacts in the atmosphere to generate an EAS. The EAS is composed mostly of electrons, positrons, and gamma rays. The electrons and the positrons emit Cerenkov light as they traverse the water in Milagro. (Cerenkov light is emitted by a charged particle traveling faster than the speed of light in a medium and is similar to a sonic boom.) The gamma rays in the EAS convert to electrons and positrons, which then emit Cerenkov light. The resultant Cerenkov light is detected by the PMTs in the pool of water (see Figure 2). The green particles represent gamma rays; the red particles represent electrons and positrons. (Rendering courtesy of Aurore Simonnet, Scientific Illustrator, Sonoma State University, aurore@universe.sonoma.edu.)

by dust. The field can be determined by measuring the energy- and redshift-dependent absorption of TeV radiation from AGN. Direct measurements are difficult (and so far unsuccessful) because of the large and uncertain foreground fields within our galaxy. The effect of the quantum fields of the universe may be manifest as a violation of Lorentz invariance—an energy dependence of the velocity of light.[1] This effect can be observed (or limited) by measuring the time delay between photons of different energies arriving from across the universe. Bursts of gamma rays provide an excellent source for observing this effect.[2]

Figure 2. A view inside Milagro. The top layer of PMTs is located at the crossing of the grid, and the bottom layer of PMTs is halfway between the grid crossing points. In the photograph, the cover is inflated for installation.

The Milagro Observatory

A cosmic ray or gamma ray entering the earth's atmosphere interacts with atoms and nuclei and loses energy in the process. At high energies, the dominant energy-loss mechanisms are the creation of particles through nuclear interactions in the case of cosmic rays and electromagnetic interactions in the case of gamma rays. The result is a cascade of particles, or EAS. As the cascade propagates through the atmosphere, particles continue to be created until the energy per particle drops below the critical energy of 80 MeV. At this point, the energy loss of the particles becomes dominated by non-particle-creating mechanisms and the EAS begins to die. When the cascade reaches the ground, it has the shape of a rough pancake with a radius of 100 m and a thickness of 1–2 m (Figure 1). A particle cascade initiated by a gamma ray comprises electrons, positrons, and lower-energy gamma rays. A particle cascade initiated by a cosmic ray will also contain muons and some hadrons in addition to the electrons, positrons, and gamma rays.

The Milagro Observatory has 723 PMTs submerged in a six-million-gallon water reservoir. The detector is located at an altitude of 2,630 m above sea level (750 g/cm^2 atmospheric overburden). The reservoir measures 80 m × 60 m × 8 m (depth) and is covered by a light-tight barrier. Each PMT is secured by a Kevlar string to a grid of sand-filled PVC (polyvinyl chloride) pipes sitting on the bottom of the reservoir. The PMTs are arranged in two layers, each on a 2.8-m × 2.8-m grid (Figure 2). The top layer of 450 PMTs (which is under 1.4 m of water) is used primarily to reconstruct the direction of the air shower. By measuring the relative arrival time of the air shower across the array, we can reconstruct the direction of the primary cosmic ray with an accuracy of roughly 0.75°. The bottom layer of 273 PMTs (which is under 6 m of water) is used primarily to discriminate between gamma-ray-initiated air showers and hadronic air showers.

Milagro Results

Background rejection. Because hadronic cosmic rays (mainly protons) are charged, they are deflected by the magnetic fields that pervade our galaxy. Outnumbering the gamma rays by ~ 10,000 to one, they form an isotropic background over which any signal must be detected. The bottom layer of PMTs in Milagro is under a sufficient amount of water such that only the penetrating component of an EAS (muons and showering hadrons) can reach it. Because a gamma-ray-induced EAS is almost completely electromagnetic and a cosmic-ray-induced EAS contains a penetrating component of muons and showering hadrons, Miagro's ability to detect the penetrating component allows us to

reject the cosmic-ray background and therefore increases our sensitivity to gamma rays. Figure 3 shows the pattern of light in the bottom layer from three gamma-ray-induced events and three proton-induced events (from Monte Carlo simulations). The proton-induced events contain small bright clumps of light, whereas the gamma-ray-induced events have a relatively uniform, low level of illumination. We have developed a *compactness* parameter that is sensitive to this difference. Using the compactness of the events, we can reject roughly 90% of the cosmic-ray background while retaining 50% of the gamma-ray-induced events.

Observation of the Crab Nebula. The Crab Nebula was the famous supernova observed by Chinese astronomers in 1066. Since that time, it has been detected in every wavelength of astronomy, from the radio to TeV gamma rays. It was the first source to be detected in TeV gamma rays,[3] and it serves as a standard candle for the field of TeV astrophysics. It was critical for Milagro to detect the Crab Nebula and to prove the efficacy of the water Cerenkov technique and our ability to reject the cosmic-ray background. This is the first detection of any source of TeV gamma rays with an EAS array.[4] The flux that we measured from the Crab Nebula is in agreement with the previous measurements by ACTs.

TeV map of the northern hemisphere. Using the same compactness parameter that we used in the Crab Nebula study, we searched for sources of TeV gamma rays from the entire northern hemisphere. Figure 4 shows the most sensitive map to date of the entire northern hemisphere in TeV gamma rays (previous maps have only been made by Milagro and its prototype Milagrito). Notice that in addition to the Crab Nebula there is another bright region in the sky, which corresponds to the active galaxy Markarian 421. Markarian 421 consists of a super-massive black hole with a jet of relativistic particles directed at earth. This black hole has experienced several flaring episodes (in the x-ray band) during our period of observation, and the TeV emission associated with these episodes is correlated with the x-ray emission. This correlation is consistent with leptonic models of gamma-ray production. In these models, electrons are accelerated at shocks that propagate down the jet of relativistic particles that is emitted along the rotation axis; these electrons radiate synchrotron radiation as they bend in the magnetic fields present in the jet. This synchrotron radiation is responsible for the observed x-ray emission. The TeV gamma rays arise from inverse Compton reactions between the primary electrons and the synchrotron photons. Aside from the Crab Nebula and the Markarian 421 black hole, no other object in the northern hemisphere appears as bright as the Crab Nebula (or the Markarian 421) in TeV gamma rays.

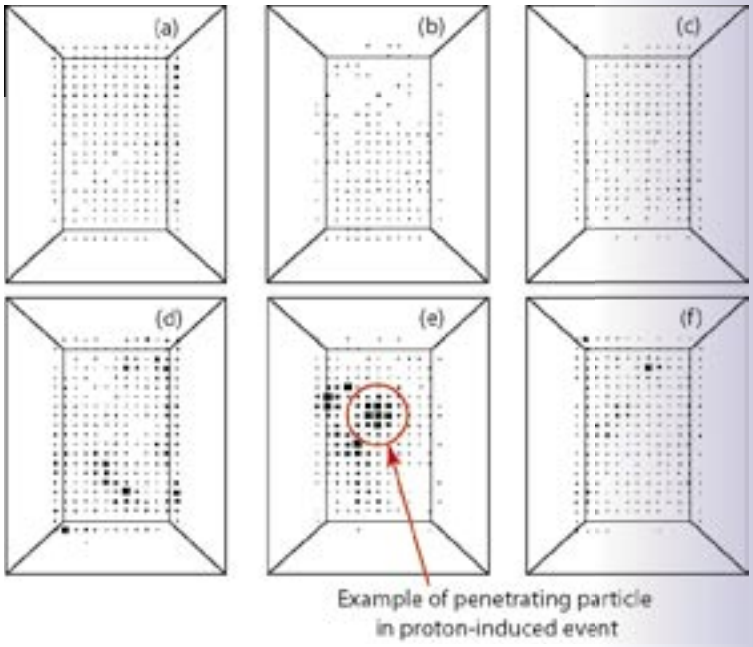

Figure 3. Monte Carlo simulations of the response of the bottom layer of detectors to EASs. The area of each square is proportional to the light level detected in a PMT. The top three events (a, b, and c) are gamma-ray induced events, and the bottom three events (d, e, and f) are proton-induced events. Clear clumps of light are observed in the proton-induced events.

Galactic-diffuse gamma rays. The origin of cosmic rays is still a matter of debate—nearly a century after their discovery! One of the clues to their origin is the energy spectrum of the gamma rays produced by the interactions of the cosmic rays with the matter in our galaxy. The highest-energy measurement of these *galactic-diffuse* gamma rays obtained to date was made by the EGRET instrument onboard the Compton Gamma Ray Observatory.[5] These measurements extend up to ~ 30 GeV and indicate an excess over predictions above several hundred MeV. The measurement of the TeV flux of the galactic-diffuse gamma rays has proven impossible to date. However, this past year Milagro has, for the first time, presented evidence of the existence of a TeV flux of gamma rays arising from interactions of cosmic rays and matter within our galaxy. Milagro has detected a signal based on the analysis of a two-year data run with a significance of 2.8 standard deviations. With another two-year run cycle on Milagro, we will be able to make a conclusive measurement of the TeV flux of galactic-diffuse gamma rays in the galaxy.

Large-scale cosmic-ray anisotropy. We generally assume that the arrival directions of cosmic rays on earth are isotropic. Milagro is the first detector that can make a high-statistics two-dimensional map of the comic-ray arrival directions. With our current data set, we can detect anisotropies as small as one part in 100,000. Figure 5 shows a two-dimensional map of the northern hemisphere in cosmic rays. This figure is similar to Figure 4, except that we have not applied our background rejection cut to the data (which increases our statistics by an order of magnitude). Moreover, we have binned the sky

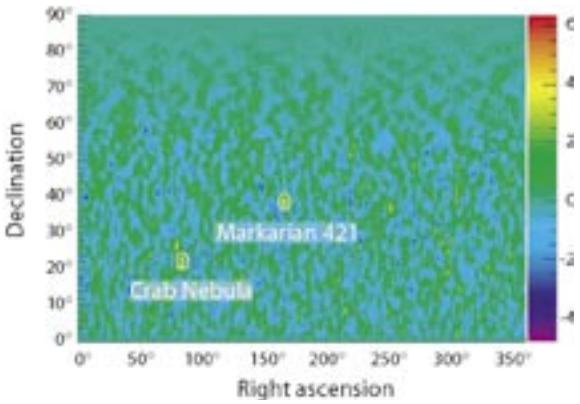

Figure 4. The northern hemisphere as seen in TeV gamma rays. Milagro is the only experiment capable of making such a plot. The two bright regions (circled and marked) are the Crab Nebula and the active galaxy, Markarian 421. The color coding corresponds to the significance of the observed excesses or deficits expressed as standard deviations.

in coarser bins to more clearly show the large-scale structure. A large-scale anisotropy is evident in this data. The red and black regions are areas with an excess of cosmic rays, and the blue regions are areas with a deficit of cosmic rays. The size of the effect is quite small (~ one part in 10,000). The origin of this anisotropy—which is currently under study—may be caused by effects of the solar magnetic field, or it may be imprinted by cosmic-ray production and propagation effects within our galaxy.

Conclusion

Milagro is the first detector of its kind—a large, water Cerenkov EAS detector. Our observations discussed above proved that the technique is sensitive to astrophysical sources of TeV gamma rays and can make measurements that no other current instrument can. Milagro will continue to operate over the next three to five years while we investigate methods to improve the instrument's sensitivity and to explore possible future detectors of a similar design. With the launch of the SWIFT satellite[6] (i.e., a detector that is sensitive to the gamma-ray, x-ray, and optical emissions from gamma-ray bursts) in 2004, Milagro's *all-sky* and *all-time* capabilities will be more important than ever before. As the only instrument capable of measuring the prompt TeV component of gamma-ray bursts, Milagro is poised to make enormous contributions to our understanding of gamma-ray bursts and perhaps of quantum gravity.

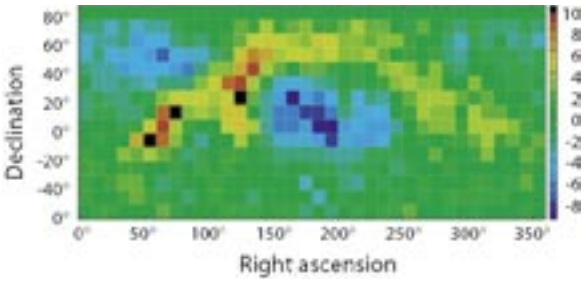

Figure 5. The northern sky as seen in TeV cosmic rays. The red to black areas represent directions from which there is an excess (over uniform) of cosmic rays, and blue regions are directions from which there is a deficit of cosmic rays.

References

1. G. Amelino-Camelia *et al.,* "Tests of quantum gravity from observations of gamma-ray bursts," *Nature* **393**, 763 (1998).
2. J. Ellis, N.E. Mavromatos, and D.V. Nanopoulos, "Search for quantum gravity," *General Relativity and Gravitation* **31**(9), 1257 (1999).
3. T.C. Weeks *et al.*, "Observation of TeV gamma rays from the Crab Nebula using the atmospheric Cerenkov imaging technique," *Astrophysical Journal* **342**, 379 (1989).
4. R. Atkins *et al.,* "Observation of TeV gamma rays from the Crab Nebula with Milagro using a new background rejection technique," *Astrophysical Journal* **595** (2003).
5. S.D. Hunter *et al.,* "EGRET observations of the diffuse gamma-ray emission from the galactic plane," *Astrophysical Journal* **481**, 205 (1997).
6. See http://swift.gsfc.nasa.gov/.

Acknowledgment

We acknowledge Scott Delay and Michael Schneider for their dedicated efforts in the construction and maintenance of the Milagro experiment. This work has been supported by grants from the National Science Foundation, including PHY-0070927, PHY-0070933, PHY-0075326, PHY-0096256, PHY-0097315, PHY-0206656, PHY-0302000, and ATM-0002744; the DOE Office of High-Energy Physics and Office of Nuclear Physics; LANL; the University of California; and the Institute of Geophysics and Planetary Physics.

For more information, contact Gus Sinnis at 505-665-6943, gus@lanl.gov.

The PHENIX Silicon Vertex Tracker Project

H.M. van Hecke, G.J. Kunde, D.M. Lee, M. Leitch, P. McGaughey (P-25), V. Ciancolo, K. Read (Oak Ridge National Laboratory), A. Drees, J. Heuser (Stony Brook University), H. En'yo, N. Saito, K. Tanida, J. Tojo [RIKEN (The Institute of Physical and Chemical Research), Japan], Y. Goto (RIKEN Brookhaven National Laboratory Research Center), N. Grau, J. Hill, J. Lajoie, C.A. Ogilvie, H. Ohnishi, H. Pei, J. Rak, G. Tuttle (Iowa State University, Ames), J. Haggerty, V. Rykov, S. White, C. Woody (Brookhaven National Laboratory), M. Togawa (Kyoto University)

A state of matter not seen in the universe since the first few microseconds after the Big Bang is the object of study of an international community of physicists at RHIC, the Relativistic Heavy-Ion Collider at BNL. When the universe was too hot for even protons and neutrons to form, it consisted almost entirely of a soup of truly elementary particles: quarks and gluons that mediate the force between the quarks. Under the conditions that prevailed for this brief span of time, quarks and gluons were free to roam. As this quark-gluon plasma (QGP) expanded and cooled, the quarks and gluons joined up to form the protons and neutrons that are part of ordinary matter today. Ever since this transition from quark matter to so-called hadronic matter, quarks have been confined to the interior of particles that we can observe.

Relativistic Heavy-Ion Collider

The RHIC complex is an accelerator/collider that can produce two counter-rotating beams of gold ions, with each beam accelerated to an energy of 100 GeV (billion electron volts) per nucleon. Thus in a head-on collision between two ions, almost 40,000 GeV of energy is available. For a fleeting instant, conditions in the collision region are thought to be sufficient to form the QGP. These collisions occur at four locations around the 2.4-mile RHIC ring; at each location, experimental apparatus observe/detect the end products of these events. The largest of these experiments is PHENIX (Figure 1).

Besides gold ions, the RHIC complex can also accelerate lighter ions, as well as deuterons (the nuclei of deuterium atoms) and protons. Studies of deuteron-gold and proton-proton collisions are necessary for the proper interpretation of the larger gold-gold events. Finally, RHIC can collide polarized, or spin-oriented, protons—enabling the study of fundamental issues related to proton spin.

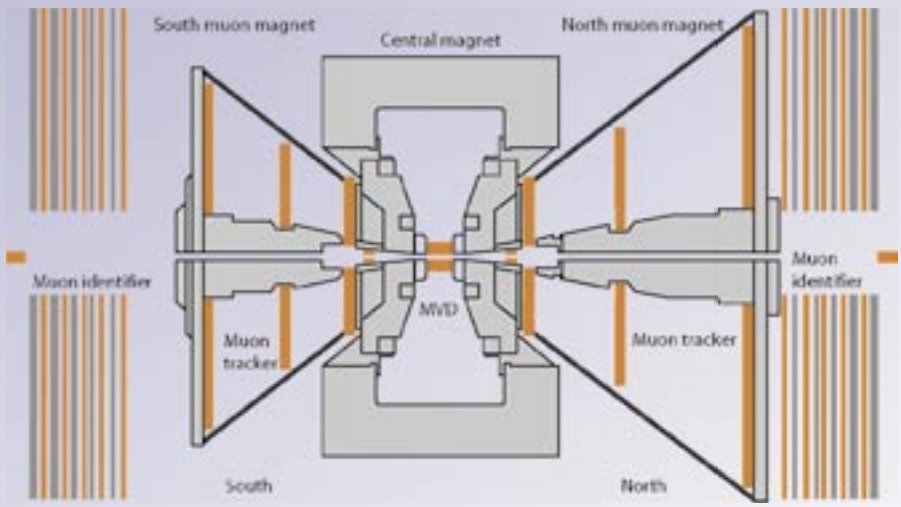

Figure 1. Side view of the PHENIX detector. Beams enter from the left and right and collide in the center. The new silicon vertex tracker will replace the multiplicity/vertex detector (MVD) in the center. Note the north and south muon magnets with three layers of tracking each. The horizontal size is 15 m. (Not shown are detectors wrapping around the collision point on the east and west side of the central magnet.)

PHENIX

The PHENIX experiment is a multipurpose detector of high-energy nuclear interactions, consisting of many different detector types. PHENIX can measure the global distribution of the thousands of particles that are produced in a gold-gold collision. These global measures can be used to determine the "centrality" of the collision—whether the ions barely grazed each other or if it was a head-on collision. The global observables also tell us, for the most central collisions, that the densities reached are many times the normal nuclear density and that these particles come blasting out at two-thirds the speed of light [at a temperature of 140 to 170 MeV, (equivalent to 10^{12}K)]. These observations indicate that the conditions for the formation of the QGP indeed exist in these events, but because the bulk of these particles are formed late in the collision, these global measures cannot give us a direct look at the earlier, hotter stages.

Hard Probes

To get a closer glimpse of the QGP, if it is indeed formed early on, the study of so-called hard probes is necessary. These can be particles that formed very early in the event and then escaped relatively unaffected by the subsequent evolution of the collision. One class of hard probes is the heavy quarks, charm and beauty (the light ones being up, down, and strange). One way to observe these heavy-quark states is to look for one of their characteristic decay modes into muons. PHENIX has a major muon-detection system, largely designed and built by LANL. Data taken in 2003 will yield results on the production of the J/ψ particle, a charm-anticharm bound state. One problem that arises in the study of muons from heavy quarks is that many other processes can produce muons. A property of the heavy-quark mesons (D mesons that contain one charm quark and B mesons that contain one beauty quark) can be exploited in this context: these particles live long enough—before decaying into muons—to travel a significant distance away from the collision point, of an order of tens or hundreds of microns. Thus the decay-muon track will appear to originate from a "secondary vertex." Our strategy, therefore, is to build a tracking detector with sufficient resolution to be sensitive to this decay distance, so that the muons from charm- and beauty-flavored mesons can be separated from the background muon sources.

Figure 2. View of one-half of the silicon vertex tracker, surrounding the beam pipe. Visible in the center are the four concentric half cylinders of the central barrel. At either end are the endcap sections, containing four conical disks each. The diameter is 40 cm, and the length is 80 cm.

The Silicon Vertex Tracker

We have embarked on a project to build a silicon vertex tracker that will be installed in the PHENIX detector in the next five years. Figure 2 shows a cutaway drawing of this detector, which wraps around the beam pipe. Beam particles circulate through the pipe in both directions, and collisions occur near the center of the silicon vertex tracker.

The silicon vertex tracker consists of a central section and two endcaps. In the central section, four concentric silicon barrels will locate the event vertex and pick up secondary vertices of tracks roughly transverse to the beam direction. The particles headed towards the muon arms are more parallel to the beam direction and are tracked by silicon detectors in two sets of disks or lampshades that cover the muon arm acceptance.

LANL has taken on the design and hopes to lead the construction of these silicon endcaps, as well as the responsibility for the overall mechanical structure of the silicon vertex tracker. This structure will be designed and built in collaboration with HYTEC, Inc., a local company that has extensive experience in similar projects. The design requirements are stringent because the detector must be built to close mechanical tolerances but must also be as light as possible. The structure shown in Figure 2 is made of fiber-reinforced polymer and carbon-carbon composite materials, and it meets the design requirements.

To achieve the required track resolution, the silicon in the endcaps will be segmented radially into 50-μm-wide strips and azimuthally into 96 segments. Strip sizes will range from 50 × 2000 μm nearest the beam pipe to 50 × 11,000 μm at the outside perimeter. We plan on using existing

Figure 3. Front (left) and back (right) view of a carbon-composite panel (brown) with four mounted silicon detectors (blue).

technology for the silicon sensors. Silicon pixel designs from the ALICE, ATLAS, or CMS experiments at CERN, the European Laboratory for Particle Physics, can be modified to match the strip sizes that we need. Developing the masks for this effort will be done in concert with the vendors of the CERN sensors, and lengthy and costly research and development in this area is not necessary.

A conceptual design for the layout of the silicon disks, or lampshades, is shown in Figures 3 and 4. Carbon-composite panels (brown) carry four silicon detectors each (blue)—two on the front and two on the back. The silicon detectors on the front and back have small overlaps, so that the final assembly will have no gaps in the coverage. A complete lampshade consists of 24 panels.

The silicon detectors are segmented along the long dimension into 50-μm-high strips, which, in turn, are split along the center line. The readout chips (not shown) are placed directly over the centerline and bonded to the strips on both sides. Signals from the smallest silicon strips at the narrow end of these assemblies are carried to the outer perimeter on kapton cables (yellow strips in Figure 3).

For the readout electronics, we similarly plan to rely heavily on existing research and development projects. We can adapt chip designs developed at FNAL for the proposed BTeV experiment to match our silicon detectors on the input end and the requirements of the PHENIX data-acquisition system on the output end. Figure 5 shows a chip layout developed from existing components. The left side of the figure shows the logical layout of the chip: two parallel arrays of electronics with signals processed from the outside in. Green is the area where the chip is bonded to the silicon strips. Red is the area reserved for preamplification and discrimination of the signals, orange is pipeline circuitry, and yellow is for digital-signal processing.

The bonding locations are staggered, as shown in Figure 5 on the right. This allows us to use a connection technology called bump-bonding, with widely spaced bumps, thereby avoiding technological hurdles associated with dense bump-bonding patterns.

These chips are 13 mm tall. So, three, five, or six of them need to be chained together lengthwise to service the different silicon detectors. One special feature of the readout-chip design is that the chip itself has power and signal bus lines running from the (green) bonding areas on the top and bottom of each chip, allowing them to be chained together. In this manner, no additional cable is needed to carry communication signals and power from each readout chip to the perimeter of the lampshades. This design simplifies construction and keeps the total mass of the device down.

Figure 4. Four lampshades, spaced 6 cm apart, each consisting of 24 panel assemblies, make up one silicon endcap.

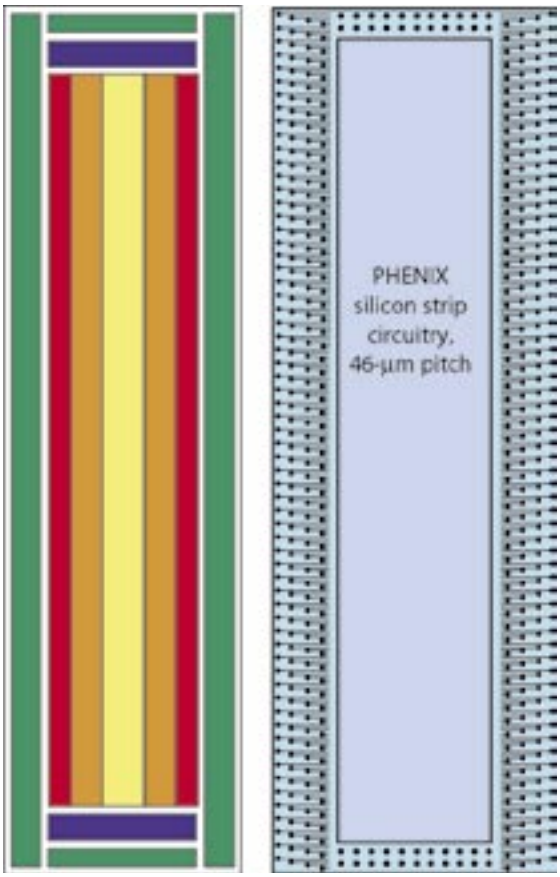

Figure 5. The logical layout of the readout chip is displayed on the left. Green is the bonding area, blue is the programming interface, red is the preamp/discriminator, orange is the pipeline, and yellow is the digital processing and signal bus. The bump-bond pattern of the chip is displayed on the right. The chip measures 3.8 mm × 13 mm and services 2 × 256 strips.

Conclusion

We have embarked on a project to extend the physics reach of the PHENIX experiment through the study of charm and beauty signals. Plans call for research and development on the silicon-vertex-tracker endcaps to continue through 2006 and for construction to proceed for the two years following. The first data taken with the new device are expected in late 2008.

Acknowledgment

I would like to thank Dave Lee and Pat McGaughey for help in the preparation of this article. The LANL silicon-vertex-tracker effort was supported by LDRD funding.

For further information, contact Hubert van Hecke at 505-667-5384, hubert@lanl.gov. For more detailed information on the silicon-vertex-tracker project, visit the project website at http://p25ext.lanl.gov/~hubert/phenix/silicon/.

Theoretical Research on Strong, Electromagnetic, and Weak Interactions

M.B. Johnson (P-25), J. Raufeisen (P-25)

In addition to the fundamental experiments conducted in P-25, we have a strong theory component consisting of a staff member, a postdoctoral fellow, and a number of short- and medium-term visitors from universities and laboratories throughout the world. Theoretical research focuses on basic issues of strong, electromagnetic-, and weak-interaction topics; these topics complement our current experimental activity and impact possible future scientific directions in the group. As such, our theoretical team is involved in both experimental and theoretical activities in the nuclear- and particle-physics community and contributes to a balanced scientific atmosphere within P-25. Recent theoretical activity has focused on parity violation in chaotic nuclei, deep inelastic and Drell-Yan reactions on nucleons and nuclei, QCD at finite temperatures, and phase transitions in the early universe.

Our analyses of Drell-Yan data from FNAL have been used to quantify how quarks propagating in nuclei lose energy and gain transverse momentum. They are based on a light-cone, target-rest-frame approach. This approach has the advantage over previous analyses in that the contribution of the shadowing of quarks is calculated rather than fit to data. Results show that both energy loss and momentum broadening of quarks occur at a rate greater than previously expected. For example, Figure 1 shows a preliminary, parameter-free, theoretical prediction of the transverse momentum distribution of the dileptons in the Drell-Yan reaction, which is based on a color-dipole representation of the quark-nucleon interaction. The result is consistent with a rate of momentum broadening about twice the currently accepted value.

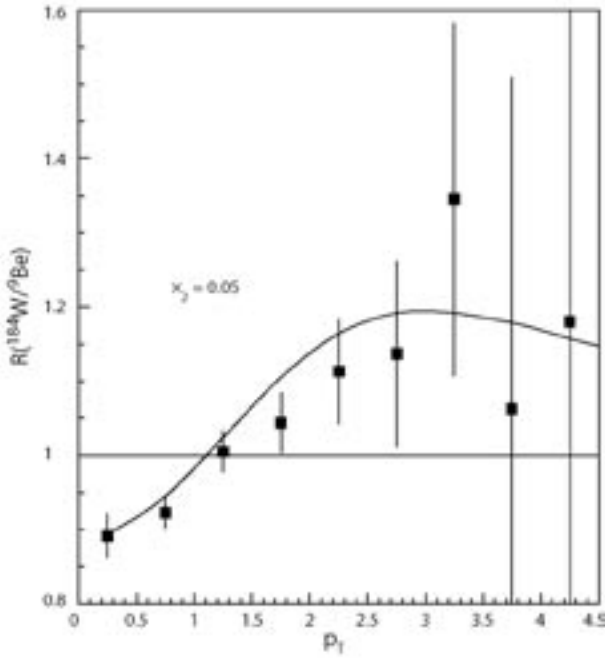

Figure 1. Comparison of theoretical prediction of $R^{W/Be}(p_T)$ versus p_T (in GeV/c) to experiment for $x_2 = 0.05$. Data are from the FNAL E772/E866 collaboration.

Radio-Frequency Emission from a Pulsed Reactor

R.E. Kelly (P-22), K.V. Lindsay (NIS-10)

In anticipating the possible move of the TA-18 nuclear reactor, an experimental and theoretical effort is under way to investigate the initiation, propagation, and detection of electromagnetic radiation in the rf portion of the spectrum resulting from a pulsed reactor. Several source mechanisms are under theoretical investigation, including bremsstrahlung, transition radiation, neutron interactions, and fission-fragment time-dependent charge exchange. The experimental method consists mainly of using various antennas, such as triaxial dipoles, monopoles, and loops. In addition, surface B-dots and D-dots and current transformers have been installed to detect possible surface waves that are guided by any conductor from the reactor environment. All measurements are in the near field due to the emitted long wavelengths. Although the project is in its initial stage, theory predicts, and experiments verify (via Fourier transforms), a continuous low-frequency emission. In addition, the instrumentation output duplicates those of the nuclear detectors in displaying the fission pulse shape. Several new experiments are planned in parallel with theoretical predictions to support potential applications.

Solid Oxygen as an Ultra-Cold Neutron Source

C.-Y. Liu (P-23), A. Saunders, C. Morris, G.E. Hogan (P-25), J.C. Long (LANSCE-3)

Following our previous success with a solid-deuterium-based UCN source at LANSCE, our team is pursuing an experimental study on another promising material, solid oxygen, for intense UCN production. The physics of UCN production in solid oxygen, involving magnon (spin wave) exchanges, is fundamentally different from the well-known phonon mechanism in solid deuterium and has the potential to produce a UCN-flux output several orders of magnitude greater than that for solid deuterium. In the solid-oxygen mechanism, the neutrons are down-scattered through coupling to the magnons in the antiferromagnetic phase of the solid—the strength of which is comparable to the nuclear scattering (phonon) in solid deuterium. This mechanism has several advantages. For one, the smaller nuclear-absorption cross section of oxygen leads to a much longer UCN lifetime in this material. Also, the UCN loss due to the absorption of the excess energy from paramolecules (a major source of loss in solid deuterium) is absent in oxygen. The UCN density achievable should be about an order of magnitude greater than that for solid deuterium. Furthermore, a factor-of-ten gain in source volume should be possible by taking advantage of the much smaller neutron-absorption probability and the infinite elastic-scattering mean-free path of a UCN in solid oxygen.

The optimal solid-oxygen operational temperature is 2 K, somewhat lower than that of solid deuterium (5 K). Nevertheless, the experiment requires minimal modification of the existing prototype solid-deuterium UCN source, mainly the extension of the cryostat capability to 2 K. Currently, we are designing such a cryostat with variable-temperature and -cooling-surface-area capabilities. Using this cryostat, we plan to carry out a comprehensive study of UCN production in solid oxygen using the LANSCE proton beam next year.

Education and Outreach

J.F. Amann (P-25)

P-25 group members continue to be active in education and outreach activities, both as participants in programs sponsored by LANL and as individual citizens who volunteer their time for various activities. Recent group-member activities include visiting classrooms for a weekly science hour and maintaining a website for this activity at http://users.hubwest.com/hubert/mrscience/science1.html. We also coordinated, organized, and participated in the "Teacher's Day" event at the annual meeting of the American Physical Society's Division of Nuclear Physics. Members of our group are technical recruiters for LANL; our recruiters visit college campuses and organize targeted recruiting activities at scientific meetings. In addition to these outreach activities, P-25 sponsors several high school, undergraduate, and graduate students to work on projects within the group (Figure 2). Through their individual schools, these students study physics, computing, engineering, and electromechanical technical support. They also supplement their learning through interactions with LANL mentors and through real on-site experience. Several students are writing theses based on the work they do at P-25.

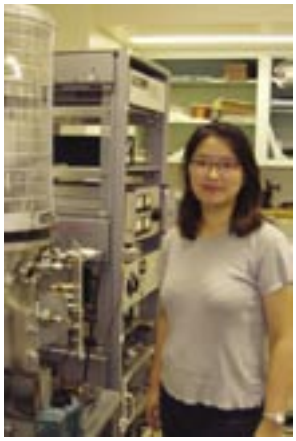

Figure 2. On September 4, 2003, the Rosen Prize Committee of the LANSCE User Group announced the selection of Chen-Yu Liu, Princeton University (now a post-doctoral appointee in P-23) as the 19th Louis Rosen Prize recipient for her outstanding Ph.D. thesis, "A Superthermal Ultra-Cold Neutron Source." Chen-Yu Liu is a member of the UCN team, a collaborative effort between P-23, P-25, Princeton University, North Carolina State University, California Institute of Technology, the Institut Laue-Langevin, Virginia Polytechnic Institute and State University, the University of Kyoto, and the Petersburg Institute for Nuclear Physics. The Rosen Prize is awarded to the student with the best thesis based on work done in whole or in large part at LANSCE.

Alpha-Dot Experiment

J.R. Torgerson, S.K. Lamoreaux, F.G. Omenetto, M.M. Schauer, and W.T. Buttler (P-23)

It has long been understood that our physical theories are incomplete descriptions of nature. An idea that is seeing renewed interest within the physics community is that this incompleteness may be manifest in space-time variation of the fine structure constant (alpha, α). One experimental effort, which compared quasar spectra to theoretical analyses of atomic structure, has suggested that a time variation of $\dot{\alpha}/\alpha = 6 \times 10^{-16}$/year may exist. This is in contrast to an analysis of the natural nuclear reactor which existed in the Oklo natural reactor in Gabon, Africa, two billion years ago and suggests that $\dot{\alpha}/\alpha < 10^{-17}$/year.

This last year, we developed two experimental plans to pursue a search for the time variation of α. The first involves the comparison of three atomic optical-frequency standards based upon trapped ions. The particular ions, In^+, Tl^+, and Yb^{2+}, are insensitive to field shifts and also have very different sensitivities to changes in α. This comparison has the potential to achieve a sensitivity to changes in α of $\delta(\dot{\alpha}/\alpha) \approx 10^{-18}$/year for a series of short measurements spanning a year. We developed a collaboration with the research group of Dmity Budker at the University of California, Berkeley; the theory group of Victor Flambaum at the University of New South Wales (Sydney); and Scott Diddams and coworkers at NIST in Boulder, Colorado. We also successfully pursued LDRD funding to support this effort for the next three years.

We are pursuing the second experimental effort in collaboration with the University of California, Berkeley; it involves a dysprosium atomic-beam apparatus. Atomic dysprosium possesses two nearly degenerate energy levels with opposite parity that exhibit a sensitivity similar to Tl^+ and Yb^{2+}. However, the levels of interest are nearly degenerate, which allows us to use rf spectroscopy rather than optical-frequency metrology—significantly easing our experimental requirements. Our experiment should achieve a sensitivity better than $\delta(\dot{\alpha}/\alpha) \approx 10^{-16}$/year within the next two years and has the potential to achieve a sensitivity of nearly $\delta(\dot{\alpha}/\alpha) \approx 10^{-18}$/year for measurements during a single year. This experiment

has recently received additional funding through a NIST Precision Measurements Grant. Finally, we reanalyzed the Oklo natural reactor data with a more realistic model for the neutron spectrum within a functioning reactor; this new analysis suggests statistically significant deviation from $\dot{\alpha} = 0$ at $\dot{\alpha}/\alpha = 2 \times 10^{-17}$/year and has inspired others to reinvestigate their own work regarding the Oklo natural reactor.

Plasma Astrophysics on the Flowing Magnetized Plasma Experiment

Z. Wang, C.W. Barnes, P.D. Beinke, S.C. Hsu, E.R. Mignardot, C. Munson, G.A. Wurden (P-24), D.C. Barnes, H. Li (X-1), K. Noguchi, X. Tang (T-15), R. Santillo (College of New Jersey), M. Martin (Texas A&M)

It is well recognized that magnetic fields can change motion of plasmas in the universe and cause structure formation on galactic (and smaller) scales. We have been building the first dedicated plasma experimental facility [the Flowing Magnetized Plasma (FMP) facility] that takes advantage of existing LANL resources and expertise to study how magnetic fields can affect plasma flow and how plasma flow, such as rotation, can be modified by magnetic field (one example is the magneto-rotational instability). The expected results will lead to a better understanding of astrophysical phenomena and their underlying physics. Such understanding can also be useful to fusion-energy research, whereby the role of plasma flows has attracted more and more attention. The experimental design and construction are guided by close interaction with theoretical and computational study.

The initial phase of construction is finished. We have constructed of a capacitor-bank system that can deliver up to 300 kJ of energy for 10 ms. The main FMP vacuum tank has achieved the base vacuum in the target regime of a few × 10^{-6} torr with 1,000 l/s turbomolecular pumps. FMP solenoids have delivered an axial, dc magnetic field up to 500 G. Theoretical studies on magneto-rotational instability caused by couette flow point out the regime of interests for our experiments. In addition to the capacitor-bank-energy-sustained plasma flow (couette flow), we also successfully created a helicon plasma that will be used to benchmark and test diagnostics for plasma flow and magnetic field.

Through a unique design of a Penning-trap-like magnetic-field structure inside the coaxial gun, we have achieved consistent plasma breakdown with as low as a 400-V capacitor-bank voltage. This is much smaller than previously reported numbers of 1 to 5 kV. The low-voltage breakdown allowed us to create a 4-ms-long pulse plasma with modest capacitor-bank energy of 60 to 100 kJ. The FMP plasma has been diagnosed with Rogowski coils, Pearson transformers, a Mach probe, a Phantom fast-framing camera, and several channels of B-dot probes. The gun-plasma peak power ranges from 10 to 40 MW depending on the capacitor-bank voltage. Thirty to fifty percent of the capacitor-bank energy is observed to convert into plasma energy (coaxial-gun current and voltage product integrated for the duration of the plasma lifetime). Initial Mach data analysis showed plasma flow on the order of 0.1–0.5 times the ion sonic speed. Both plasma imaging and B-dot measurements indicate interesting plasma self-organization and structure-formation processes, which give rise to magnetic fields in both the axial and azimuthal directions in the cylindrical geometry of the FMP.

Search for a Permanent Electric Dipole Moment of the Electron Using a Paramagnetic Crystal

C.-Y. Liu, S.K. Lamoreaux (P-23), M.A. Espy, A. Matlachov (P-21)

As it is free from hadronic uncertainties, the EDM of the electron can be used to make direct measurements of (or set limits on) the interaction strength of new particles postulated by popular extensions to the Standard Model. The sensitivity of current EDM measurements is approaching that of several predictions for new physics. We are carrying out one such high-sensitivity search for the electron EDM. This search uses a solid-state system, and hence it promises orders-of-magnitude improvement over atomic beams solely from the available electron density. An electrically insulating paramagnetic material will become spin-polarized in the presence of an electric field, if an electron EDM exists. For an electron EDM even many times smaller than the current limit, the polarized sample develops a net magnetization that can be detected with high sensitivity using state-of-the-art SQUID

magnetometers. This electric-field-induced spin-order increases as the sample temperature decreases. We are studying gadolinium gallium garnet (GGG) that has a low conductivity and a high concentration of heavy ions, Gd^{3+}, as a candidate material for this experiment. The gadolinium ion, in the garnet crystal field, is predicted to have an EDM 2.2 times that of the bare electron. Using a practical sample size of 100 cm^3 and a typical high electric field of 10 kV/cm, we expect, after 10 days of data averaging, to place an experimental limit on the electron EDM on the level of 10^{-29} *e*cm (electron-centimeters). This is 100 times more sensitive than the current limit set by the thallium atomic-beam experiment at the University of California, Berkeley.

Over the past year, we have synthesized large polycrystalline GGG samples (using the solid-state reaction method) in our laboratory. We have performed a series of sample characterizations using x-ray scattering and magnetic susceptibility measurements below 4 K. We have designed and constructed the experimental apparatus, which includes high-voltage electrodes, a magnetic-shielding package, a SQUID gradiometer, and a liquid-helium cryostat. Currently, we are testing a large-capacity dilution refrigerator, an essential component of this experiment, which will be used to cool the whole assembly to below 100 mK. We expect to perform systematic studies this winter and produce preliminary results on the electron EDM next year.

High-Energy Nuclear Physics

D.M. Lee (P-25), representing the PHENIX collaboration

An important area of study in P-25 is the distribution of partons in nucleons and nuclei. This includes the nuclear modification of QCD processes such as the production of J/ψ particles (made up of a charm/anticharm quark pair). We are continuing to publish research on this topic from a program centered at FNAL, where we have performed measurements of Drell-Yan and heavy-quark production in fixed-target proton-nucleus collisions since 1987. Our most recent measurement from the NuSea Experiment (E866) is an analysis of the absolute Drell-Yan cross sections in p-p and p-d collisions at 800 GeV/c. This is the first measurement of the Drell-Yan cross section in p-p collisions over a broad kinematic range and the most extensive study of p-d collisions. A detailed comparison with recent global parton distribution fits is in good agreement for the light antiquark sea, but the parton fits overestimate the valence quark distributions as Bjorken-x approaches 1.

Our new proposal (E906), titled "Drell-Yan Measurements of Nucleon and Nuclear Structure with the FNAL Main Injector," aims to improve on the E866 measurement of the ratio of anti-d/anti-u quarks, with coverage to much larger values of Bjorken-x. E906 has been approved by the FNAL program-advisory committee and a formal funding proposal has been submitted to DOE. Approximately $3 million was requested for the construction of a new large-dipole magnet and additional detector construction funds. E906 is currently scheduled to begin taking data in 2008. The recently installed and commissioned muon arms at PHENIX are well poised to continue these studies. Measurements of J/ψ production in p-p and d-Au collisions at $\sqrt{S} = 200$ GeV are currently under way.

The Majorana Experiment

S.R. Elliott (P-23), representing the Majorana collaboration

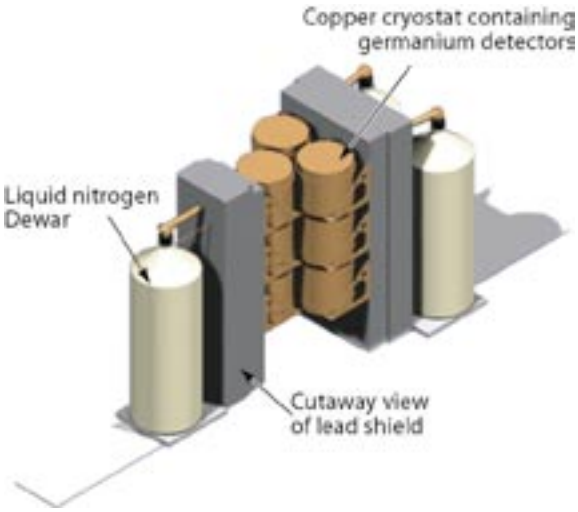

Figure 3. A cut-away concept drawing for the proposed Majorana apparatus.

The objective of the Majorana experiment (Figure 3) is to study neutrinoless double beta decay ($0\nu\beta\beta$) with an effective Majorana-neutrino mass sensitivity below 50 meV to characterize the Majorana nature of the neutrino, the neutrino mass spectrum, and the absolute mass scale. An experimental study of the neutrino mass scale implied by neutrino oscillation results is now technically within our grasp. This exciting physics goal is best pursued using the well-established technique of searching for $0\nu\beta\beta$ of ^{76}Ge, augmented with recent advances in signal processing and detector design. The Majorana experiment will consist of a large mass of ^{76}Ge in the form of high-resolution intrinsic germanium detectors located deep underground within a low-background shielding environment. Observation of a sharp peak at the $\beta\beta$ endpoint will quantify the $0\nu\beta\beta$ half-life and thus the effective Majorana mass of the electron neutrino. The collaboration has recently finished a draft proposal to build and operate this experiment.

The Majorana proposal is based on well-established technology that does not require proof-of-principle research and development. However, there are two research and development projects that are currently under way to optimize the engineering design of the Majorana experiment. These projects are called SEGA (segmented enriched germanium assembly) and MEGA (multiple element germanium array). Not only do these efforts help to optimize the Majorana design, but they will also achieve physics goals in and of themselves. The goal of SEGA is to optimize the previously successful, signal-processing techniques for crystals whose charge collection is segmented. The goal of MEGA is to optimize the arrangement and packaging for multiple crystals sharing a single cooling system. For the Majorana experiment, we will implement the optimum configuration determined by the SEGA and MEGA activities and operate with a large quantity of enriched germanium material to reach a significant sensitivity for the $0\nu\beta\beta$ half-life.

Wide-Angle Cerenkov Telescope

G. Sinnis, B.L. Dingus, F. Samuelson, X. Xu (P-23), R. Atkins (University of Wisconsin), J. A. Goodman (University of Maryland), L.A. Kelley, D.A. Williams (University of California, Santa Cruz), G. Mohanty (University of California, Riverside), T. Stephens, S. Stochaj (New Mexico State University), G.B. Yodh (University of California, Irvine)

The origin of cosmic rays is still a mystery 100 years after their discovery. An important clue to their origin lies in their nuclear composition. Beyond an energy of ~ 100 TeV, the composition cannot be directly measured from space but must be inferred from indirect, ground-based measurements. To date, no ground-based technique has been able to measure the composition of the cosmic rays in an energy regime (< 100 TeV) where direct measurements have been performed. This has left the veracity of conflicting ground-based measurements in question.

The WACT is an array of six atmospheric Cerenkov telescopes, each equipped with a fast camera (composed of 25 PMTs) that measures the lateral distribution of the Cerenkov light generated by EASs. The lateral distribution of the shower light is sensitive to the altitude at which the air shower reaches its greatest development (shower maximum). Shower maximum is, in turn, dependent upon the nuclear species of the primary cosmic ray—lighter nuclei such as protons have a smaller cross section and therefore penetrate deeper into the atmosphere. During the past year, WACT has acquired over 10,000 high-quality events that are currently undergoing analysis.

Qweak: A Precision Measurement of the Proton's Weak Charge

G.S. Mitchell, J.D. Bowman, S.I. Penttilä, W.S. Wilburn (P-23), and the Qweak collaboration

The Qweak experiment (Figure 4) at the Thomas Jefferson National Accelerator Facility (JLab) aims to make a 4% measurement of the parity-violating asymmetry in elastic scattering at very low Q^2 of a longitudinally polarized electron beam on a proton target. The experiment will measure the weak charge of the proton (and thus the weak mixing angle at low-energy scale), providing a precision test of the Standard Model. Because the value of the weak mixing angle ($\sin^2\theta_w$) is approximately one-quarter, the weak charge of the proton ($Q_w^p = 1 - 4\sin^2\theta_w$) is suppressed in the Standard Model, making it especially sensitive to the value of the mixing angle and also to possible new physics. The experiment is approved to run at JLab, and the construction plan calls for the hardware to be ready to install in Hall C in 2007. The experiment will be a 2,200-hour measurement, employing an 80% polarized, 180-μA, 1.2-GeV electron beam; a 35-cm liquid-hydrogen target; and a toroidal magnet to focus electrons scattered at 9°, which is a small forward angle corresponding to $Q^2 = 0.03$ $(GeV/c)^2$. With these kinematics, the systematic uncertainties from hadronic processes are strongly suppressed. To obtain the necessary statistics, the experiment must run at an event rate of over 6 GHz. This requires current mode detection of the scattered electrons, which will be achieved with synthetic-quartz Cerenkov detectors. We will use a tracking system in a low-rate counting mode to determine average Q^2 and the dilution factor of background events.

LANL members of the Qweak collaboration are responsible for the design and construction of the quartz detector system. The expected event rate for scattered electrons of 760 MHz per detector octant precludes counting the individual events. Instead, the experiment will use current-mode detection and low-noise, front-end electronics, which are areas of technical expertise of the LANL collaborators. Preliminary design work and prototype testing has begun at LANL. Simulations indicate that the detector design will be sufficient to produce 50 photoelectrons per event in the photomultiplier at each end of each quartz bar, a level which will allow the collection of data to be limited only by counting statistics.

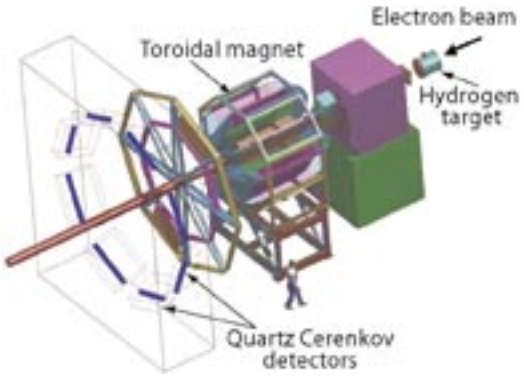

Figure 4. Conceptual design for the Qweak experimental setup in Hall C at JLab. The electron beam (1.2 GeV, 180 μA, P = 80%, 30 Hz reversal) enters the experimental apparatus at the upper right (at the 35-cm-long liquid hydrogen target and scattering chamber). The eight current-mode, synthetic-quartz Cerenkov detectors (~ 6-GHz total rate) are each 2 m × 12 cm × 2.5 cm. The spectrometer provides clean separation of elastic and inelastic electrons at its focal plane.

Pulsed-Cold Neutron Beta Decay

W.S. Wilburn, J.D. Bowman, G.S. Mitchell, S.I. Penttilä, P.-N. Seo (P-23), J.M. O'Donnell (LANSCE-3)

The beta (β) decay of the neutron provides one of the most sensitive tests of the Standard Model of electroweak interactions. The neutron, which consists of two down quarks and one up quark, is converted into a proton, which consists of one down quark and two up quarks. During the decay process, an electron and an electron-type anti-neutrino are created. Precise measurements of various decay parameters (including correlations between the momenta of the decay particles and the initial neutron spin) and of the shape of the electron energy spectrum are sensitive to the physics of the electroweak interaction. Previous measurements have been consistent with present theory; however, the most precise measurements obtained from the most recent β-decay experiment differ from theory by three standard deviations. Previous measurements have been limited by systematic errors.

We are developing a new experimental approach that uses a pulsed-cold neutron beam like the current one at LANSCE and the one planned for the Spallation Neutron Source at Oak Ridge National Laboratory (ORNL). Our approach incorporates two key technologies: an existing ^{3}He spin-filter neutron polarizer and a new spectrometer with two large-area silicon detectors having thin dead layers on either end (Figure 5). (Our team has been developing the new spectrometer.) Combining a pulsed-cold neutron beam and a ^{3}He spin-filter neutron polarizer allows us to determine neutron polarization with unprecedented accuracy. The new spectrometer will allow us to detect both the proton and electron events from each neutron β decay in coincidence—thus greatly reducing background noise. All sources of systematic errors that have limited the sensitivity of previous experiments to approximately 1% are expected to be less than 0.1% with our approach; these effects are monitored by *in situ* checks. If successful, this spectrometer-development work will lead to an important experimental program at LANL.

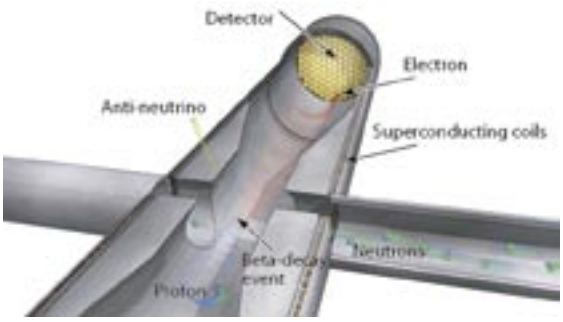

Figure 5. A cut-away drawing of the neutron-beta-decay spectrometer. A neutron-beta-decay event is shown with the newly created proton and electron spiraling toward opposite detectors under the influence of the spectrometer's magnetic field. One of the two silicon detectors is visible.

In the past year, we have made progress on several fronts. The preliminary design of the spectrometer is at a point where an engineering design can begin. The design achieves the required magnetic field and homogeneity and allows for adiabatic transport of the polarized neutrons into the decay region. We have worked closely with silicon-detector manufacturers and now have a quote for producing a suitable prototype spectrometer. The silicon detectors will be 4 in. in diameter and 2 mm thick with thin dead layers. In addition, the detectors will be capable of withstanding high-bias voltages to achieve high charge-carrier drift velocities. An apparatus has been constructed at LANL to measure the timing resolution of the two silicon detectors. It consists of an ^{90}Sr β source; a thin, fast, plastic scintillator that will provide a timing fiducial signal; and a vacuum chamber with a cold finger (i.e., a cooled cooper rod that conducts heat away from the silicon detectors) for mounting and cooling the silicon detectors to 80 K. Working with our collaborators at ORNL and a company with expertise in designing analog-to-digital converters (ADCs), we now have a working concept of how to digitize the detector signals while preserving energy and timing information. The ADC modules sample at 100 MHz and include a sophisticated field-programmable gate array and a digital-signal processor to handle the high data rates on board.

The PHENIX Program at RHIC

D.M. Lee, P.D. Barnes, J.G. Boissevain, M.L. Brooks, J. Burward-Hoy, G.J. Kunde, M.J. Leitch, M.X. Liu, P.L. McGaughey, J.M. Moss, D.O. Silvermyr, W.E. Sondheim, J.P. Sullivan, H.W. van Hecke (P-25)

Members of Group P-25 are developing innovative technology for a large international program at BNL's RHIC aimed at helping researchers better understand the subatomic physics that defined the early universe. "Big Bang" cosmology pictures a time very early in the evolution of the universe when the density of quarks and gluons was so large that they existed as a plasma; they were not confined in the hadrons we know today (neutrons, protons, pions, and related particles). A large international research team—known as the PHENIX collaboration—is attempting to produce a small sample of this primordial QGP in the laboratory and to study its exotic properties. (The PHENIX collaboration includes about 500 physicists and engineers from universities and laboratories in the U.S. and in 14 foreign countries.) The challenge facing this team is to identify the fleeting transition from two colliding gold beams to this de-confined phase of matter, QGP, using the PHENIX collider detector (Figure 6) at the RHIC. Los Alamos plays a major role in defining both the search for the QGP and the related physics program at RHIC. To help realize this goal, researchers and engineers from P-25 are constructing major subsystems for PHENIX—an MVD and two muon spectrometers.

The MVD is the smallest and among the most technically complex of the PHENIX subsystems. It surrounds the interaction region where two beams of 200-GeV/nucleon ions collide. The functions of the MVD are to determine the precise location of the interaction vertex where the transition to the QGP should occur and to measure the global distribution and total number of secondary charged particles; these properties are crucial parameters used to determine the energy density achieved in the collision fireball. A fully instrumented MVD has been installed and is now taking data during the physics runs of PHENIX. The muon spectrometers, the largest subsystem on PHENIX, consist of two conically shaped radial field magnets on opposite ends of the PHENIX detector, with three stations of position-sensitive tracking chambers inside the magnets. These chambers are the largest of their kind in the world. The muon subsystem plays a central role in P-25's physics agenda because it is optimized for examining hard-scattering observables at very high temperatures and densities, where the strong force is smaller and easier to calculate using a method known as "perturbative quantum chromodynamics." Both spectrometers are completely installed and are presently taking data. Analysis of the recorded data shows clear mass peaks for the J/Psi resonance, which will help researchers determine if the QGP exists—a keystone of the PHENIX physics program and a clear demonstration of the successful operation of the muon-spectrometer systems.

Figure 6. Rendering of the PHENIX collider detector.

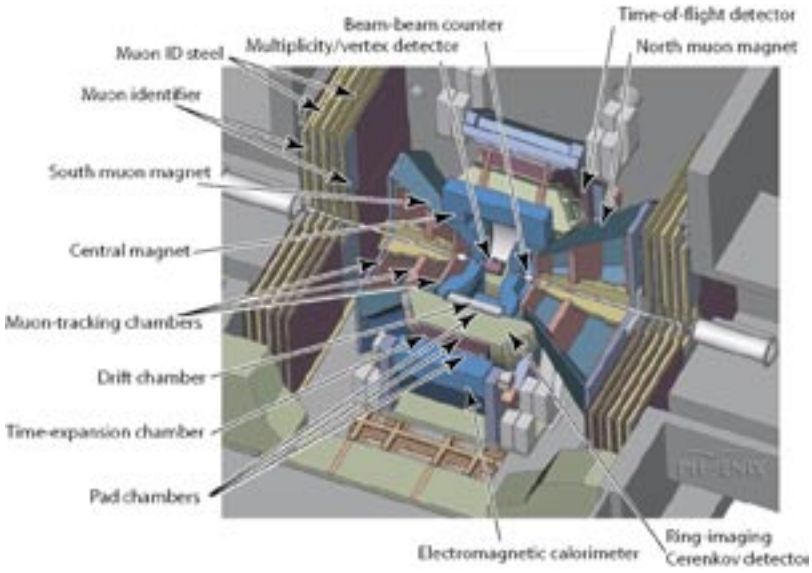

Neutron-Beta-Decay-Asymmetry Measurement Using the New Ultra-Cold Neutron Source at LANL

A. Saunders (P-25), representing the UCN-A collaboration

An experiment is under construction at LANL that will measure the angular correlation between the neutron spin and the direction of emission of the electron in polarized neutron beta (β) decay, which is characterized by the coefficient *A* and is usually called the β asymmetry of neutron decay. A measurement of the β asymmetry involves a determination of the forward-backward asymmetry of the β with respect to the direction of the neutron polarization. A measurement of *A*, when combined with knowledge of the neutron lifetime, provides a determination of the fundamental-vector and axial-vector weak coupling constants. Previous measurements of *A* have disagreed both among themselves and with other measurements of the vector weak coupling constant and with the requirement of the Standard Model that the Cabibbo-Kobayashi-Maskawi (CKM) matrix be unitary. In short, a β-asymmetry measurement provides a sensitive means to search for physics beyond the Standard Model (such as right-handed currents)—phenomena that are predicted to occur in a number of Grand Unified Field Theories (GUTs).

The new experiment at LANL will measure the β asymmetry of the decay of ultracold neutrons (UCNs). UCNs provide a uniquely sensitive tool for this kind of measurement, because they can be held for long periods of time in storage bottles and guide systems and also because they can be polarized to close to 100% polarization using the $\vec{\mu} \cdot \vec{B}$ potential. The first property allows them to be created in a high-radiation environment then piped to a very-low-background environment for the measurement, and the second property allows UCN measurements on polarized neutrons to achieve lower systematic uncertainties caused by the neutron polarization than other techniques. Because UCNs have temperatures of only about a milli-Kelvin, UCN experiments in the past have typically been limited by the available density of neutrons. Therefore, an important part of the LANL work has been to design and construct a new UCN source capable of supplying much higher densities of neutrons to an experiment.

The UCN source and experiment are being built at the Los Alamos Neutron Science Center (LANSCE). An overhead view of the layout of the new facility is shown in Figure 7. The source is designed to produce the neutrons using a 4-μA beam of 800-MeV protons from the LANSCE accelerator; it therefore lies behind a shield package consisting of about 5000 tons of steel behind a 6-ft layer of concrete. The UCNs are piped out through the wall of the shield package using special quartz guides coated with a diamond-like carbon coating—chosen for the high velocity of neutrons that they can guide and for the low probability of losing a neutron when it collides with the wall of the guide. The experiment consists of a 7-T superconducting solenoid magnet to polarize the UCNs, another 1-T magnet to maintain the UCN polarization and guide the β-decay particles to detector stacks, and other associated guide and calibration hardware.

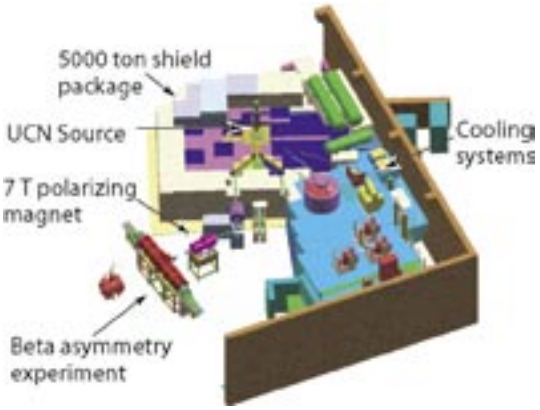

Figure 7. Experimental Area B at LANSCE showing the installation of the new UCN source, associated cooling systems, and the experiment that will use the UCNs to measure the neutron-β-decay asymmetry. Installation of the systems shown is nearing completion.

The UCN source uses a solid-deuterium converter to produce the UCNs through a nonequilibrium superthermal process in which more UCNs are produced than would be expected from the Maxwell-Boltzman distribution at the temperature of the moderator. This technology has been developed over the last few years at LANL by this team and has resulted in a new understanding of the physics of UCN interactions with solid deuterium, a prototype UCN source that produced a greater density of UCNs than any other existing UCN source, and also a design for a full-scale source that is predicted to produce even more UCNs. Construction of the new source and experiment are nearly complete; all the major components are on site and are now being installed in the experimental area at LANSCE. First beam on target is expected in early 2004, with first measurements of neutron-β-decay asymmetry expected shortly thereafter.

Gamma-Ray Burst Science

M.M. Gonzalez, B.L. Dingus (P-23), Y. Kaneko, R.D. Preece, M.S. Briggs (University of Alabama, Huntsville), C.D. Dermer (Naval Research Laboratory)

Using archival data taken by EGRET and BATSE (both of which are instruments on board the Compton Gamma Ray Observatory satellite), team members have searched for a new high-energy component to gamma-ray burst emission. Of 24 bursts examined, they found one burst with just such a component. This work was published in *Nature,* and the lead author, Maria Gonzalez (a graduate student in P-23), received an award from the Los Alamos Awards Program for her work.

Existing models of high-energy particle production in gamma-ray bursts cannot explain the existence of this spectral component; it appears that the acceleration of protons in gamma-ray bursts is needed to explain this result. This gives credence to the idea that gamma-ray bursts may be the source of UHECRs.

Spin Physics at RHIC

D.M. Lee (P-25), representing the PHENIX collaboration

The muon detectors at PHENIX are also designed to study which subatomic components of the proton carry its spin. When both beams at the RHIC are composed of polarized protons, the p-p interactions are directly sensitive to the fraction of spin carried by the gluons. The measurements of heavy-quark and quarkonium production through muon channels are one of the most promising tools to directly probe the polarized-gluon structure function inside the proton. During 2001 and 2002, we successfully measured J/ψ production with the newly installed south muon detector from the first polarized p-p collisions at RHIC.

Previous deep-inelastic-scattering measurements were only sensitive to the sum of the quark and antiquark contributions to the proton spin. However, by using polarized proton beams to induce the Drell-Yan process, it will be possible for the first time to separately determine the spin of the antiquarks. Additionally, by measuring the asymmetry of the charge states of the intermediate-vector boson (W), the flavor dependence (i.e., the difference between up- and down-quark contributions to the spin) can be extracted. There is no doubt that the RHIC spin program will produce exciting physics results as the polarization and luminosity improve in the coming years.